Summer 2017

Boundary integral equation based numerical solutions of helmholtz transmission problems for composite scatters

Haiyang Qi
New Jersey Institute of Technology

Copyright Warning & Restrictions

The copyright law of the United States (Title 17, United States Code) governs the making of photocopies or other reproductions of copyrighted material.

Under certain conditions specified in the law, libraries and archives are authorized to furnish a photocopy or other reproduction. One of these specified conditions is that the photocopy or reproduction is not to be "used for any purpose other than private study, scholarship, or research." If a, user makes a request for, or later uses, a photocopy or reproduction for purposes in excess of "fair use" that user may be liable for copyright infringement,

This institution reserves the right to refuse to accept a copying order if, in its judgment, fulfillment of the order would involve violation of copyright law.

Please Note: The author retains the copyright while the New Jersey Institute of Technology reserves the right to distribute this thesis or dissertation

Printing note: If you do not wish to print this page, then select "Pages from: first page # to: last page #" on the print dialog screen

ABSTRACT

BOUNDARY INTEGRAL EQUATION BASED NUMERICAL SOLUTIONS OF HELMHOLTZ TRANSMISSION PROBLEMS FOR COMPOSITE SCATTERS

by
Haiyang Qi

In this dissertation, an in-depth comparison between boundary integral equation solvers and Domain Decomposition Methods (DDM) for frequency domain Helmholtz transmission problems in composite two-dimensional media is presented. Composite media are characterized by piece-wise constant material properties (i.e., index of refraction) and thus, they exhibit interfaces of material discontinuity and multiple junctions. Whenever possible to use, boundary integral methods for solution of Helmholtz boundary value problems are computationally advantageous. Indeed, in addition to the dimensional reduction and straightforward enforcement of the radiation conditions that these methods enjoy, they do not suffer from the pollution effect present in volumetric discretization. The reformulation of Helmholtz transmission problems in composite media in terms of boundary integral equations *via* multi-traces constitutes one of the recent success stories in the boundary integral equation community. Multi-trace formulations (MTF) incorporate local Dirichlet and Neumann traces on subdomains within Green's identities and use restriction and extension by zero operators to enforce the intradomain continuity of the fields and fluxes. Through usage of subdomain Calderon projectors, the transmission problem is cast into a linear system form whose unknowns are local Dirichlet and Neumann traces (two such traces per interface of material discontinuity) and whose operator matrix consists of diagonal block boundary integral operators associated with the subdomains and extension/projections off diagonal blocks. This particular form of the matrix operator associated with MTF is amenable to operator preconditioning *via* Calderon projectors.

DDM rely on subdomain solutions that are matched *via* transmission conditions on the subdomain interfaces that are equivalent to the physical continuity of fields and traces. By choosing the appropriate transmission conditions, the convergence of DDM for frequency domain scattering problems can be accelerated. Traditionally, the intradomain transmission conditions were chosen to be the classical outgoing Robin/impedance boundary conditions. When the ensuing DDM linear system is solved *via* Krylov subspace methods, the convergence of DDM with classical Robin transmission conditions is slow and adversely affected by the number of subdomains. Heuristically, this behavior is explained by the fact that Robin boundary conditions are first order approximations of transparent boundary conditions, and thus there is significant information that is reflected back into a given subdomain from adjacent subdomains. Clearly, using more sophisticated transparent boundary conditions facilitates the information exchange between subdomains. For instance, Dirichlet-to-Neumann (DtN) operators of adjacent domains or suitable approximations of these can be used in the form of generalized Robin boundary conditions to increase the rate of the convergence of iterative solvers of DDM linear systems. The approximations of DtN operators that are expressed in terms of Helmholtz hypersingular operators (e.g., the normal derivative of the double layer operator) are used in this dissertation. The incorporation of these in a DDM framework is subtle, and an effective method is proposed to blend these transmission operators in the presence of multiple junctions. Conceptually, the information exchange between subdomains is realized through certain Robin-to-Robin (RtR) operators, which how to compute robustly *via* integral equation formulations is shown.

All of the Helmholtz boundary integral operators that feature in Calderon's calculus are discretized *via* Nyström methods that rely on sigmoid transforms, trigonometric interpolation, and singular kernel splitting. Sigmoid transforms are means to polynomially accumulate discretization points toward corners without

compromising the discretization density in smooth boundary portions. A wide variety of numerical results is presented in this dissertation that illustrate the merits of each of the two approaches (MTF and DDM) for the solution of transmission problems in composite domains.

BOUNDARY INTEGRAL EQUATION BASED NUMERICAL SOLUTIONS OF HELMHOLTZ TRANSMISSION PROBLEMS FOR COMPOSITE SCATTERS

by
Haiyang Qi

A Dissertation
Submitted to the Faculty of
New Jersey Institute of Technology and
Rutgers, The State University of New Jersey – Newark
in Partial Fulfillment of the Requirements for the Degree of
Doctor of Philosophy in Mathematical Sciences

Department of Mathematical Sciences
Department of Mathematics and Computer Science, Rutgers-Newark

August 2017

APPROVAL PAGE

BOUNDARY INTEGRAL EQUATION BASED NUMERICAL SOLUTIONS OF HELMHOLTZ TRANSMISSION PROBLEMS FOR COMPOSITE SCATTERS

Haiyang Qi

Catalin C. Turc, Dissertation Advisor — Date
Associate Professor of Mathematics, NJIT

Dr. Michael S. Siegel, Committee Member — Date
Professor of Mathematics, NJIT

Dr. Zoi-Heleni Michalopoulou, Committee Member — Date
Professor of Mathematics, NJIT

Dr. Peter G. Petropoulos, Committee Member — Date
Associate Professor of Mathematics, NJIT

Dr. Francisco-Javier Sayas, Committee Member — Date
Professor of Mathematics, University of Delaware

BIOGRAPHICAL SKETCH

Author: Haiyang Qi

Degree: Doctor of Philosophy

Date: August 2017

Undergraduate and Graduate Education:

- Doctor of Philosophy in Mathematical Sciences,
  New Jersey Institute of Technology, Newark, NJ, 2017
- Bachelor of Science in Computational Mathematics
  Jilin University, Changchun, P.R. China, 2012

Major: Mathematical Sciences

I would like to dedicate this thesis to my parents Qi Zhao and Liu Hua, who have been doing the utmost to support me in all these years. I want to thank them for their love and care. Although these years we are in different countries and I didn't have much time with them, their contributions to my life will be felt and remembered forever

ACKNOWLEDGMENT

I would like to gratefully thank Professor Catalin Turc, who expertly guided me through my graduate education and led me to finish the research. He has been an excellent mentor and teacher. Also, my appreciation extends to all the professors who taught me these years. I learned a lot from them. I want to thank Prof. Michael S. Siegel, Prof. Zoi-Heleni Michalopoulou, Prof. Peter G. Petropoulos, Prof. Francisco-Javier Sayas for being on my committee.

I want to thank my college mates and friends, Pejman, Peter, Rui, Emel, RJ and so on, who helped me in different aspects during these years, from class to daily life. I spent a good and fun time with you guys.

And last, I would like to express gratitude toward the staff in the department of Mathematics and NJIT. Their work helped me to finish my graduate education successfully.

TABLE OF CONTENTS

LIST OF TABLES

LIST OF FIGURES

CHAPTER 1

INTRODUCTION

The electromagnetic scattering by bounded penetrable objects composed of several subdomains with different but constant electric permittivities is relevant for numerous applications in antenna design, diffraction gratings, and photovoltaic cells, to name but a few. In these cases, it is typical that multiple media meet at a single point, a scenario that is referred to as multiple junctions. Numerical methods for the solution of scattering from large frequency range composite objects with piecewise constant material parameters need to resolve wave interactions with high-contrast sharp interfaces, which is challenging numerically. Volumetric discretizations of these problems result in very large systems of equations that are ill-conditioned in the high-frequency regime and whose solution by iterative solvers require inordinate numbers of iterations. Several preconditioning strategies have been proposed to mitigate the above issue, the most successful arguably being those that rely on the shifted Laplacean [2, 11] or the sweeping preconditioner introduced in [10].

Domain Decomposition Methods (DDM) are natural candidates for the solution of scattering problems involving composite scatterers. DDM are divide and conquer strategies whereby the computational domain is divided into smaller subdomains and subdomain solutions are matched *via* transmission conditions on the subdomain interfaces. The convergence of DDM for frequency domain scattering applications depends a great deal on the choice of the transmission conditions that allow the exchange of information between adjacent subdomains. These interface transmission conditions should ideally allow information to flow out of a subdomain with as little as possible information being reflected back into the subdomain. Thus, the interface transmission conditions fall into the category of Absorbing Boundary Conditions

(ABC). From this perspective, the ideal choice of transmission conditions on an interface between two subdomains is such that the impedance/transmission operator is the restriction to the common interface of the Dirichlet to Neumann (DtN) operator corresponding to the adjacent subdomain. Traditionally, the interface transmission conditions were chosen as the classical (first order ABC) outgoing Robin/impedance boundary conditions [8, 14]. The convergence of DDM with the classical Robin interface boundary conditions is slow and is adversely affected by the number of subdomains. The convergence of DDM can be considerably improved through incorporation of ABC that constitute higher order approximations of DtN operators in the form of second order approximations with optimized tangential derivative coefficients [13], square root approximations [3], or other types of non-local transmission conditions [14, 23]. Alternatively, PML can be used at subdomain interfaces [24]. Although the use of more sophisticated ABC recounted above accelerates a great deal the convergence of DDM, the number of iterations required for convergence still grows (albeit not drastically) with the frequency and number of subdomains. This is not entirely surprising since the higher order ABC described above only concern local exchange of information between adjacent subdomains, and affect to a lesser degree the global exchange of information between distant subdomains. Recent efforts have been devoted to construct "double sweep" type preconditioners that address the latter issue [27, 28]. The resulting preconditioned DDM scale favorably with the frequency and number of subdomains, but appear to be somewhat less effective for wave propagation problems in composite media that exhibit sharp high-contrast interfaces.

Boundary integral equation based solvers for scattering by composite objects with piecewise constant material properties require significantly fewer unknowns than volumetric solvers as only the interfaces of material discontinuity need be discretized. The formulation of these problems in terms of robust boundary integral equations has

recently received significant interest in the community, the main achievement being the introduction of Multitrace formulations [15, 5]. The derivation of one of the multitrace formulation consists of the following steps: (1) use of Green's identities in each subdomain (whose boundary is a union of interfaces of material discontinuity) to represent the fields in that subdomain *via* layer potential; (2) application of Dirichlet and Neumann traces associated to that subdomain to the Green's identities, followed by (3) enforcement of the continuity conditions across interfaces to replace the identity terms in the previous steps by Dirichlet and Neumann traces of solutions in adjacent subdomains. This procedure leads to a boundary integral equation of the first kind whose unknowns are both interior and exterior Dirichlet and Neumann traces of fields on each interface and which involves (in the scalar case) the four boundary integral operators on each subdomain corresponding to the wavenumber associated with that subdomain. The multitrace formulation of the second kind can be derived if the fields are sought in terms of suitable linear combinations of layer potentials defined on the union of all interfaces of material discontinuity (typically referred to as the skeleton).

Our dissertation work seeks to investigate the performance of Nyström solvers based multitrace formulations and DDM solvers in the case of high-frequency scattering problems from composite high contrast scatterers. A major advantage of multitrace formulation is the ease with which they can be incorporated into existing boundary integral equation solvers. We present in this work a straightforward extension of the Helmholtz transmission Nyström solvers introduced in [9] to multitrace formulations. We also investigate a simple Calderón preconditioner for the multitrace formulation of the first kind. This preconditioner is shown to be effective for high-frequency high-contrast scattering problems from composite scatterers. However, the numbers of iterations required by Nyström discretizations of multitrace formulations grows considerably with the frequency and/or the contrast between subdomains, even after resorting to preconditioning. We show that in the

aforementioned frequency regime DDM based on boundary integral equations can be advantageous alternatives to multitrace formulations. We investigate both DDM based on the exchange of classical Robin data between subdomain. We solve the subdomain Helmholtz equations with Robin using well-conditioned boundary integral formulations solved by Nyström discretizations. Provided the size of the subdomains is small enough (in terms of wavelengths across), the latter problems can be solved by direct linear algebra methods.

The lay out of the dissertation is as follows. In Chapter 2, we formulate the Helmholtz transmission problems in the case of one subdomain, we review the four boundary integral operators associated with the Helmholtz equation and their mapping properties, and we review the classical boundary integral equation of the second kind for the solution of transmission problems. In Chapter 3, we discuss several versions of DDM for the solution of Helmholtz transmission problems; the various choices correspond to various choices of transmission operators. In Chapter 4, we discuss strategies to compute the RtR maps that are at the heart of DDM; all of these methods rely on boundary integral formulations. We also discuss in Chapter 4 the well-posedness of the DDM with several choices of transmission operators. In Chapter 5, we state the transmission problem in composite domains. In Chapter 6, we review the Multi-Trace Formulation of transmission problems in composite domains with piece-wise continuous material properties. In Chapter 7, we present several versions of DDM for transmission problems in composite domains with piece-wise continuous material properties and we garner insight on the spectral properties of these DDM in the one-dimensional case. In Chapter 8, we present Nyström discretizations of the four boundary integral operators associated with the Helmholtz equation and we describe how to use them in order to build discretizations of MTF and various DDM. Finally, in Chapter 9, we present numerous numerical results that compare the iterative behavior of the MTF and DDM formulations.

CHAPTER 2

SCALAR TRANSMISSION PROBLEMS

We consider the problem of two dimensional transmission by structures that feature partial coatings, i.e., penetrable scattering problems when parts of the boundary of the scatterer are perfectly conducting/impenetrable. Let Ω_1 denote a bounded domain in $\mathbb{R}^2$ whose boundary $\Gamma := \partial\Omega_1$ is given locally by the graph of a Lipschitz function, and let $\Omega_0 := \mathbb{R}^2 \setminus \Omega_1$. We seek to find fields u_0 and u_1 that are solutions of the following scalar Helmholtz transmission problem:

$$\begin{aligned} \Delta u_j + k_j^2 u_j &= 0 && \text{in} \quad \Omega_j, \\ u_0 + u^{inc} &= u_1 && \text{on} \quad \Gamma, \\ \alpha_0(\partial_{n_0} u_0 + \partial_{n_0} u^{inc}) &= -\alpha_1 \partial_{n_1} u_1 && \text{on} \quad \Gamma_T, \\ \lim_{r\to\infty} r^{1/2}(\partial u_0/\partial r - ik_0 u_0) &= 0. \end{aligned} \tag{2.1}$$

We assume that the wavenumbers k_j and the quantities α_j in the subdomains Ω_j are positive real numbers. The unit normal to the boundary $\partial\Omega_j$ is here denoted by n_j and is assumed to point to the exterior of the subdomain Ω_j. The incident field u^{inc}, on the other hand, is assumed to satisfy the Helmholtz equation with wavenumber k_0 in the unbounded domain Ω_0. Finally, we assume that the parameters α_j are positive so that the transmission problem (2.1) is well posed. We present next arguments that establish the uniqueness of solutions of transmission problems (2.1). The uniqueness is establish once we show that the only solution of the system (2.1) with $u^{inc} = 0$ is the trivial solution. The main argument relies on a result [6] that will be used several times throughout this text.

Lemma 2.0.1 *If w is a radiative solution of the Helmholtz equation in the unbounded domain Ω_0 corresponding to a positive wavenumber that satisfies*

$$\Im \int_\Gamma \overline{\partial_{n_0} w}\ w\ ds \leq 0$$

then $w = 0$ in Ω_0.

The uniqueness argument proceeds by observing that

$$\Im \int_\Gamma \overline{\partial_{n_0} u_0}\ u_0\ ds = -\frac{\alpha_1}{\alpha_0} \Im \int_\Gamma \overline{\partial_{n_1} u_1}\ u_1\ ds = -\frac{\alpha_1}{\alpha_0} \Im \int_{\Omega_1} |\nabla u_1|^2 - k_1^2 |u_1|\ dx = 0.$$

The existence of solution of the system (2.1) will be establish *via* boundary integral equation arguments. In what follows, we review two main formulations of the transmission problem (2.1). One such formulation relies on boundary integral equations, while the other is a domain decomposition method.

We start with the definition of the single and double layer potentials. Given a wavenumber k and a density φ defined on Γ, we define the single layer potential as

$$[SL_k(\varphi)](\mathbf{z}) := \int_\Gamma G_k(\mathbf{z} - \mathbf{y}) \varphi(\mathbf{y}) ds(\mathbf{y}), \mathbf{z} \in \mathbb{R}^2 \setminus \Gamma \tag{2.2}$$

and the double layer potential as

$$[DL_k(\varphi)](\mathbf{z}) := \int_\Gamma \frac{\partial G_k(\mathbf{z} - \mathbf{y})}{\partial \mathbf{n}(\mathbf{y})} \varphi(\mathbf{y}) ds(\mathbf{y}), \mathbf{z} \in \mathbb{R}^2 \setminus \Gamma \tag{2.3}$$

where $G_k(\mathbf{x}) = \frac{i}{4} H_0^{(1)}(k|\mathbf{x}|)$ represents the two-dimensional Green's function of the Helmholtz equation with wavenumber k. H_0^1 is the Hankel function of order zero of the first kind. We denote by γ_D^j and γ_N^j the $\Omega_j, j = 0, 1$ Dirichlet and respectively Neumann traces (taken with respect to the exterior unit normal n_j, j=0,1) on Γ. We will also use the notation *int* to denote the domain Ω_1 and *ext* to denote the domain Ω_0. Applying these traces to the single and double layer potentials corresponding to

the wavenumber k and a density φ we have

$$\begin{aligned}
\gamma_D^j SL_k(\varphi) &= S_k\varphi \\
\gamma_N^j SL_k(\varphi) &= \frac{\varphi}{2} + K_k^\top \varphi \\
\gamma_D^j DL_k(\varphi) &= -\frac{\varphi}{2} + K_k\varphi \\
\gamma_N^1 DL_k(\varphi) &= \gamma_N^2 DL_k(\varphi) = N_k\varphi.
\end{aligned} \tag{2.4}$$

In Equation (2.4) the operators K_k and $K_k^\top$, usually referred to as double and adjoint double layer operators, are defined for a given wavenumber k and density φ as

$$(K_k\varphi)(\mathbf{x}) := \int_\Gamma \frac{\partial G_k(\mathbf{x}-\mathbf{y})}{\partial \mathbf{n}(\mathbf{y})}\varphi(\mathbf{y})ds(\mathbf{y}),\ \mathbf{x} \text{ on } \Gamma \tag{2.5}$$

and

$$(K_k^\top\varphi)(\mathbf{x}) := \int_\Gamma \frac{\partial G_k(\mathbf{x}-\mathbf{y})}{\partial \mathbf{n}(\mathbf{x})}\varphi(\mathbf{y})ds(\mathbf{y}),\ \mathbf{x} \text{ on } \Gamma. \tag{2.6}$$

Furthermore, for a given wavenumber k and density φ, the operator N_k denotes the Neumann trace of the double layer potential on Γ given in terms of a Hadamard Finite Part (FP) integral which can be re-expressed in terms of a Cauchy Principal Value (PV) integral that involves the tangential derivative ∂_s on the curve Γ

$$\begin{aligned}
(N_k\varphi)(\mathbf{x}) &:= \text{FP}\int_\Gamma \frac{\partial^2 G_k(\mathbf{x}-\mathbf{y})}{\partial \mathbf{n}(\mathbf{x})\partial \mathbf{n}(\mathbf{y})}\varphi(\mathbf{y})ds(\mathbf{y}) \\
&= k^2\int_\Gamma G_k(\mathbf{x}-\mathbf{y})(\mathbf{n}(\mathbf{x})\cdot\mathbf{n}(\mathbf{y}))\varphi(\mathbf{y})ds(\mathbf{y}) \\
&+ \text{PV}\int_\Gamma \partial_s G_k(\mathbf{x}-\mathbf{y})\partial_s\varphi(\mathbf{y})ds(\mathbf{y}).
\end{aligned}$$

Finally, the single layer operator S_k is defined for a wavenumber k as

$$(S_k\varphi)(\mathbf{x}) := \int_\Gamma G_k(\mathbf{x}-\mathbf{y})\varphi(\mathbf{y})ds(\mathbf{y}),\ \mathbf{x} \text{ on } \Gamma \tag{2.7}$$

for a density function φ defined on Γ.

Green identities can be now written in the simple form:

$$u_j = SL_{k_j}\gamma_N^j u_j - DL_{k_j}\gamma_D^j u_j$$

Similarly,

$$C_j = \frac{1}{2}\begin{bmatrix} I & \\ & I \end{bmatrix} + (-1)^j \begin{bmatrix} -K_k & S_k \\ -N_k & K_k^T \end{bmatrix}, j = 1, 2$$

are the Calderón exterior/interior projections associated to the exterior/interior Helmholtz equation:

$$C_j^2 = C_j, C_j \begin{bmatrix} \gamma_D^j u_j \\ \gamma_N^j u_j \end{bmatrix} = \begin{bmatrix} \gamma_D^j u_j \\ \gamma_N^j u_j \end{bmatrix}$$

From these equations, we can deduce

$$S_k N_k = -\frac{1}{4}I + K_k^2, N_k S_k = -\frac{1}{4}I + (K_k^T)^2, N_k K_k = K_k^T N_k$$

We recount some important results related to the mapping properties of the four boundary integral operators of the Calderon calculus.

Theorem 2.0.2 *Let D_2 be a bounded domain, with Lipschitz boundary Γ. The following mappings*

- $S_k : H^s(\Gamma) \to H^{s+1}(\Gamma)$
- $K_k : H^{s+1}(\Gamma) \to H^{s+1}(\Gamma)$
- $K_k^\top : H^s(\Gamma) \to H^s(\Gamma)$
- $N_k : H^{s+1}(\Gamma) \to H^{s+1}(\Gamma)$

are continuous for $s \in [-1, 0]$. Furthermore, if $k_1 \neq k_2$ we have that

- $S_{k_1} - S_{k_2} : H^{-1}(\Gamma) \to H^1(\Gamma)$
- $K_{k_1} - K_{k_2} : H^0(\Gamma) \to H^1(\Gamma)$
- $K_{k_1}^\top - K_{k_2}^\top : H^{-1}(\Gamma) \to H^0(\Gamma)$
- $N_{k_1} - N_{k_2} : H^0(\Gamma) \to H^0(\Gamma)$

are continuous and compact.

We also recount a result due to Escauriaza, Fabes and Verchota [12]. In this result, K_0, $K_0^\top$ are the double and adjoint double layer operator for Laplace equation (which obviously correspond to $k = 0$).

In what follows, we replace the subindex k in the definition of the layer potentials and boundary integral operator (BIO) by the subindex j of the wavenumber k_j corresponding to the Ω_j subdomain. We also denote the BIO associated with Laplace equation (that is wavenumber is equal to zero) by using the subindex L.

Theorem 2.0.3 *For any Lipschitz curve Γ and $\lambda \notin [-1/2, 1/2)$, the mappings*

$$\lambda I + K_L : H^s(\Gamma) \to H^s(\Gamma)$$

are invertible for $s \in [-1, 1]$. Furthermore, the mappings

$$\frac{1}{2} I \pm K_L : H^s(\Gamma) \to H^s(\Gamma)$$

are Fredholm of index 0 for $s \in [-1, 1]$.

Boundary integral equation formulations of the transmission problem (5.1) can be derived using layer potentials defined on Γ: the solutions $u_j, j = 0, 1$, of the transmission problem are sought in the form

$$u_j(\mathbf{x}) := SL_{\Gamma,j}\ v + (-1)^j \alpha_j^{-1} DL_{\Gamma,j}\ p, \quad \mathbf{x} \in \Omega_j, \tag{2.8}$$

where v and p are densities defined on the Γ and the double layer operators are defined with respect to exterior unit normals $\mathbf{n}$ corresponding to each domain Ω_j. Applying the Dirichlet and Neumann traces followed by transmission conditions, we arrive at the the following pair of integral equations:

$$\begin{aligned} \tfrac{\alpha_0^{-1}+\alpha_1^{-1}}{2} p - (\alpha_0^{-1} K_0 + \alpha_1^{-1} K_1) p + (S_1 - S_0) v &= u^{inc} \\ \tfrac{\alpha_0+\alpha_1}{2} v + (N_0 - N_1) p + (\alpha_0 K_0^\top + \alpha_1 K_1^\top) v &= -\alpha_0 \frac{\partial u^{inc}}{\partial n_0} \end{aligned} \tag{2.9}$$

Note that the combination $N_0 - N_1$ occurs, this is an integral operator with a weakly-singular kernel. In what follows, we refer to the integral Equation (2.9) by CFIESK. The well posedness of the CFIESK formulation in the space $(p, v) \in H^{1/2}(\Gamma) \times H^{-1/2}(\Gamma)$ was established in [25]; we reiterate the main arguments in what follows. Clearly, we have

$$\begin{aligned} \mathcal{D} &:= \begin{bmatrix} \frac{\alpha_0^{-1}+\alpha_1^{-1}}{2} I - (\alpha_0^{-1} K_0 + \alpha_1^{-1} K_1) & (S_1 - S_0) \\ N_0 - N_1 & \frac{\alpha_0+\alpha_1}{2} I + (\alpha_0 K_0^\top + \alpha_1 K_1^\top) \end{bmatrix} \\ &= \begin{bmatrix} (\alpha_0^{-1} + \alpha_1^{-1})(\frac{1}{2} I - K_L) & 0 \\ 0 & (\alpha_0 + \alpha_1)(\frac{1}{2} I + K_L^\top) \end{bmatrix} + \mathcal{D}_c \end{aligned}$$

where the matrix operator $\mathcal{D}_C : H^{1/2}(\Gamma) \times H^{-1/2}(\Gamma) \to H^{1/2}(\Gamma) \times H^{-1/2}(\Gamma)$ is compact by the results recounted in Theorem 2.0.2. Since the principal part of the operator $\mathcal{D}$ is Fredholm of index zero, it follows that the matrix operator $\mathcal{D}$ is a compact perturbation of an operator that is Fredholm of index zero. Thus, the well-posedness of the CFIESK formulations follows once we establish the injectivity of the operator $\mathcal{D}$.

Let $(p_0, v_0) \in Ker(\mathcal{D})$ and let us define fields $u_j, j = 0, 1$ according to Formula (2.8) and densities (p_0, v_0). Obviously, the fields u_0 and u_1 are solutions of the transmission system (2.1) with zero incident field, and thus it follows that $u_1 = 0$ in Ω_1 and $u_0 = 0$ in Ω_0. Also, u_0 satisfies the Helmholtz equation in the

domain Ω_1 with wavenumber k_0, and respectively u_1 is a radiative solution of the Helmholtz equation with wavenumber k_1 in the unbounded domain Ω_0. Using the continuity properties of the layer potentials, we see that u_1 and u_0 satisfy the following system

$$\begin{aligned}
\Delta u_1 + k_1^2 u_1 &= 0 \qquad \text{in} \qquad \Omega_0, \\
\Delta u_0 + k_0^2 u_0 &= 0 \qquad \text{in} \qquad \Omega_1, \\
\alpha_0 u_0 + \alpha_1 u_1 &= 0 \qquad \text{on} \qquad \Gamma, \\
\partial_{n_1} u_0 &= \partial_{n_0} u_1 \quad \text{on} \qquad \Gamma, \\
\lim_{r\to\infty} r^{1/2}(\partial u_1/\partial r - ik_1 u_1) &= 0.
\end{aligned} \tag{2.10}$$

Again, we have

$$\Im \int_\Gamma \overline{\partial_{n_0} u_1}\; u_1 \; ds = -\frac{\alpha_0}{\alpha_1} \Im \int_\Gamma \overline{\partial_{n_1} u_0}\; u_0 \; ds = -\frac{\alpha_0}{\alpha_1} \Im \int_{\Omega_1} |\nabla u_0|^2 - k_0^2 |u_0| \; dx = 0$$

from which we conclude that $u_1 = 0$ in Ω_0 and $u_0 = 0$ in Ω_1. Consequently, we obtain that $p = 0$ and $v = 0$ on Γ, and hence, the well-posedness of CFIESK is established.

CHAPTER 3

DOMAIN DECOMPOSITION APPROACH

DDM are natural candidates for numerical solution of transmission problems (2.1). A non-overlapping domain decomposition approach for the solution of Equation (2.1) consists of solving subdomain problems in $\Omega_j, j = 0, 1$ with matching Robin transmission boundary conditions on the common subdomain interface Γ. Indeed, this procedure amounts to computing the subdomain solutions:

$$\begin{aligned} \Delta u_j + k_j^2 u_j &= 0 \quad \text{in} \quad \Omega_j, \qquad (3.1) \\ \alpha_j(\partial_{n_j} u_j + \delta_j^0 \partial_{n_j} u^{inc}) + Z_j(u_j + \delta_j^0 u^{inc}) &= -\alpha_\ell(\partial_{n_\ell} u_\ell + \delta_\ell^0 \partial_{n_\ell} u^{inc}) + Z_j(u_\ell + \delta_\ell^0 u^{inc}) \\ &\text{on} \quad \Gamma \end{aligned}$$

where $\{j, \ell\} = \{0, 1\}$ and δ_j^0 stands for the Kronecker symbol, and Z_j, Z_ℓ are transmission operators with the following mapping property $Z_{j,\ell} : H^{1/2}(\Gamma) \to H^{-1/2}(\Gamma)$. The choice of the operators Z_j, Z_ℓ should be such that the following PDEs are well posed

$$\begin{aligned} \Delta u_j + k_j^2 u_j &= 0 \text{ in } \Omega_j, \\ \alpha_j \partial_{n_j} u_j + Z_j u_j &= \psi_j \text{ on } \Gamma. \qquad (3.2) \end{aligned}$$

where we require in addition that u_0 be radiative at infinity. Sufficient condition for the well-posedness of these problems are given by

$$\pm \Im \int_\Gamma Z_1 \varphi \, \overline{\varphi} ds > 0, \qquad \Im \int_\Gamma Z_0 \varphi \, \overline{\varphi} ds < 0, \quad \text{for all } \varphi \in H^{1/2}(\Gamma), \qquad (3.3)$$

under the assumption that α_j are positive numbers. In addition, $Z_0 + Z_1 : H^{1/2}(\Gamma) \to H^{-1/2}(\Gamma)$ must be a bijective operator in order to guarantee that the solution of the

DDM system (3.1) is also a solution of the original transmission problem (2.1). In order to describe the DDM method more concisely we introduce subdomain Robin-to-Robin (RtR) maps [14]. For each subdomain $\Omega_j, j = 0, 1$ we define RtR maps $\mathcal{S}^j, j = 0, 1$ in the following manner:

$$\mathcal{S}^0(\psi_0) := (\alpha_0 \partial_{n_0} u_0 - Z_1 u_0)|_\Gamma, \qquad \mathcal{S}^1(\psi_1) := (\alpha_1 \partial_{n_1} u_1 - Z_0 u_1)|_\Gamma \tag{3.4}$$

where $u_j, j = 0, 1$ are solutions of Equation (3.2). The DDM (3.1) can be recast in terms of computing the global Robin data $f = [f_1 \ f_0]^\top$ with

$$f_j := (\alpha_j \partial_{n_j} u_j + Z_j u_j)|_\Gamma, \ j = 0, 1,$$

as the solution of the following linear system that incorporates the subdomain RtR maps $\mathcal{S}^j, j = 0, 1$, previously defined

$$(I + \mathcal{S}) f = g, \quad \mathcal{S} := \begin{bmatrix} 0 & \mathcal{S}^1 \\ \mathcal{S}^0 & 0 \end{bmatrix} \tag{3.5}$$

with right-hand side $g = [g_1 \ g_0]^\top$ wherein

$$\begin{aligned} g_1 &= (-\alpha_0 \partial_{n_0} u^{inc} + Z_1 u^{inc})|_\Gamma \\ g_0 &= -(\alpha_0 \partial_{n_0} u^{inc} + Z_0 u^{inc})|_\Gamma. \end{aligned}$$

We note that due to its possibly large size, the DDM linear system (3.5) is typically solved in practice *via* iterative methods. The behavior of iterative solvers of Equation (3.5) depends a great deal on the choice of transmsission operators $Z_j, j = 0, 1$. Ideally, these transmission operators should be chosen so that information flows out of the subdomain and no information is reflected back into the subdomain. This can be achieved if the operator Z_0 is the Dirichlet-to-Neumann (DtN) operator corresponding to the Helmholtz Equation (3.2) posed in the domain Ω_1 and viceversa [22, 16]. Since such DtN operators are not well defined for all

wavenumbers k_0 and k_1, and expensive to calculate even when properly defined, easily computable approximations of DtN maps can be employed effectively to lead to faster convergence rates of GMRES solvers for DDM algorithms [3]. For instance, the transmission operators can be chosen in the following manner [26]:

$$Z_0 = -2\alpha_1 N_{\Gamma,k_1+i\sigma_1}, \qquad Z_1 = -2\alpha_0 N_{\Gamma,k_0+i\sigma_0}, \quad \sigma_j > 0. \tag{3.6}$$

Given that hypersingular operators are, in general, expensive to compute, we proceed to replace the hypersingular operators in Equation (3.6) by principal symbol Fourier multiplier operators. The latter principal symbols are defined as

$$p^N(\xi, k_0 + i\sigma_0) = -\frac{1}{2}\sqrt{|\xi|^2 - (k_0 + i\sigma_0)^2} \quad p^N(\xi, k_1 + i\sigma_1) = -\frac{1}{2}\sqrt{|\xi|^2 - (k_1 + i\sigma_1)^2}, \tag{3.7}$$

where the square root branches are chosen such that the imaginary parts of the principal symbols are positive. The principal symbol Fourier multipliers are defined in the Fourier space $TM(\Gamma)$ [1] as

$$\left[PS(N_{\Gamma,k_j+i\sigma_j})\hat{\varphi_1}\right](\xi) = p^N(\xi, k_j + i\sigma_j)\hat{\varphi_1}(\xi) \tag{3.8}$$

for a density φ_1 defined on $\partial\Omega_1$. We define accordingly

$$Z_0^{PS} = -2\alpha_1 PS(N_{\Gamma,k_1+i\sigma_1}), \qquad Z_1^{PS} = -2\alpha_0 PS(N_{\Gamma,k_0+i\sigma_0}), \quad \sigma_j > 0. \tag{3.9}$$

and we use the operators in Equation (3.9) as transmission operators in the DDM formulation. We refer to the ensuing DDM with transmission operators defined in (3.9) as Optimized DDM (DDMO). In addition, a high-frequency approximation as $k_j \to \infty$ of the square root expressions defined in Equation (3.7) results in yet another possible choice of transmission operators

$$Z_0^a = -i\alpha_1(k_0 + i\sigma_0)I \qquad Z_1^a = -i\alpha_0(k_1 + i\sigma_1)I. \tag{3.10}$$

Heuristics on the choice of transmission operators. The intuition behind the choices above is provided in the following heuristic calculations on the RtR operators $\mathcal{S}^j$. It suffices to provide these calculations for the RtR operator $\mathcal{S}^1$, the other case being similar. If we denote by Y^1 the DtN operator corresponding to the domain Ω_1 (again, assume it is well defined), then the boundary condition can be written as

$$(\alpha_1 Y^1 + Z_1)u_1 = \psi_1$$

and thus

$$u_1 = (\alpha_1 Y^1 + Z_1)^{-1}\psi_1$$

and hence

$$\mathcal{S}^1 = I - (Z_0 + Z_1)(\alpha_1 Y^1 + Z_1)^{-1}.$$

Given that $Z_0 \approx \alpha_1 Y^1$, by which we mean that the difference between those two operators is a regularizing operators (i.e., compact), it follows that $\mathcal{S}^1$ is itself a compact operator, and so is $\mathcal{S}^0$. Thus, the DDM system is expressed as a compact perturbation of the identity operator. However, making these heuristics rigorous is difficult.

An important question is the well-posedness of the DDM system (3.5) with the aforementioned choices of transmission operators (3.6),(3.9), and (3.10). To the best of our knowledge, the first proof regarding the well-posedness of DDM with Robin transmission for Helmholtz problems condition was provided in [14] with $Z_j = i\eta,\ \eta < 0$. In that case, the RtR operators turn out to be unitary, a property that plays a crucial role in the well-posedness proof. In our case, neither of the choses recounted above (i.e., equations (3.6),(3.9), and (3.10)) leads to unitary RtR operators, and thus, the proof of well-posedness of the DDM system (3.5) should rely on different arguments.

From a practical perspective, we are interested in robust methods for the discretization of the RtR operators. We will derive three exact representations of those in terms of boundary integral operators.

CHAPTER 4

CALCULATIONS OF RTR OPERATORS IN TERMS OF BOUNDARY INTEGRAL OPERATORS

We first reformulate the RtR operators in terms of solutions of the following Helmholtz problems

$$\begin{aligned} \Delta u_j + k_j^2 u_j &= 0 \text{ in } \Omega_j, \\ \partial_{n_j} u_j + \alpha_j^{-1} Z_j u_j &= \varphi_j \text{ on } \Gamma. \end{aligned}$$

with u_0 radiative at infinity, for which

$$\mathcal{S}^0(\varphi_0) := (\partial_{n_0} u_0 - \alpha_0^{-1} Z_1 u_0)|_\Gamma, \qquad \mathcal{S}^1(\varphi_1) := (\partial_{n_1} u_1 - \alpha_1^{-1} Z_0 u_1)|_\Gamma.$$

While expressing the operator $\mathcal{S}^j, j = 0, 1$ in terms of boundary integral operators is a relatively simple task, doing it robustly turns out to be more complicated in the case of $\mathcal{S}^0$. A robust, albeit relatively complicated representation of these operators was recently introduced and analyzed in [26]. We start with Green identities

$$u_j = SL_j \partial_n u_j - DL_j u_j \qquad \text{in} \qquad D_j.$$

Applying the Dirichlet and Neumann traces on Γ corresponding to the domain Ω_j to the equation above we get

$$\begin{aligned} \frac{1}{2} u_j + K_j u_j + \alpha_j^{-1} S_j Z_j u_j &= S_j \varphi_j \\ \frac{\alpha_j^{-1} Z_j u_j}{2} - N_j u_j - \alpha_j^{-1} K_j^T Z_j u_j &= \frac{1}{2} \varphi_j - K_j^T \varphi_j. \end{aligned}$$

We add the first equation above to the second equation composed on the left with the operator $2S_{k_j + i\sigma_j}$ where $\sigma_j > 0$ and we obtain a *direct* Regularized Combined Field

Integral Equation(CFIER) of the form

$$\begin{aligned}\mathcal{A}_j(u_j|_\Gamma) &= (S_j + S_{\kappa_j} - 2S_{\kappa_j}K_j^\top)\varphi_j, \quad \kappa_j = k_j + i\sigma_j,\ \sigma_j > 0,\\ \mathcal{A}_j &:= \frac{1}{2}I - 2S_{\kappa_j}N_j + \alpha_j^{-1}S_{\kappa_j}Z_j - 2\alpha_j^{-1}S_{\kappa_j}K_j^\top Z_j + K_j + \alpha_j^{-1}S_jZ_j. \quad (4.1)\end{aligned}$$

It is a straightforward matter [26] to show that

$$\mathcal{A}_j = \alpha_j^{-1}(\alpha_0+\alpha_1)I + \alpha_j^{-1}(\alpha_j - \alpha_{j+1})K_L - 2\alpha_j^{-1}(\alpha_j + 2\alpha_{j+1})K_L^2 + 4\alpha_j^{-1}\alpha_{j+1}K_L^3 + \widetilde{\mathcal{A}_j} \quad (4.2)$$

where the operators $\widetilde{\mathcal{A}_j} : L^2(\Gamma) \to L^2(\Gamma)$ are compact for $j = 0, 1$, and $j+1 = j+1(mod 2)$. Thus, the RtR operators $\mathcal{S}^j$ can be expressed as

$$\mathcal{S}^j = I - \alpha_j^{-1}(Z_0 + Z_1)\mathcal{A}_j^{-1}(S_j + S_{\kappa_j} - 2S_{\kappa_j}K_j^\top),\ j = 0, 1. \quad (4.3)$$

As mentioned above, the operators $\mathcal{S}^1$ can be computed robustly in a much simpler manner. Indeed, we start with Green's identity

$$u_1 = -DL_1(u_1|\Gamma) + SL_1(\partial_{n_1}u_1)|_\Gamma, \qquad \text{in } \Omega_1$$

to which we apply the Dirichlet trace on Γ to derive another *direct* boundary integral equation

$$\mathcal{B}_1 u_1|_\Gamma = S_1\varphi_1, \text{ on } \Gamma, \qquad \mathcal{B}_1 u_1|_\Gamma := \left(\frac{1}{2}I + K_1 + \alpha_1^{-1}S_1Z_1\right)u_1|_\Gamma. \quad (4.4)$$

We establish the following result

Theorem 4.0.1 *The operators $\mathcal{B}_1$ defined in Equation (4.4) are invertible with continuous inverses in the spaces $H^s(\Gamma)$ for all $s \in [-1, 1]$.*

Proof. We have that

$$\begin{aligned}\mathcal{B}_1 &= \frac{1}{2}I + K_1 - 2\frac{\alpha_0}{\alpha_1}S_1N_{k_0+i\sigma_0}\\ &= \frac{1}{2}I + K_L + \frac{\alpha_0}{2\alpha_1}I - 2\frac{\alpha_0}{\alpha_1}K_L^2 + \widetilde{B}_1\\ \widetilde{\mathcal{B}_1} &:= (K_1 - K_L) - 2\frac{\alpha_0}{\alpha_1}S_1(N_{k_0+i\sigma_0} - N_L) + 2\frac{\alpha_0}{\alpha_1}(S_1 - S_L)N_L.\end{aligned}$$

Using the mapping properties recounted in Theorem 2.0.2 it follows immediately that the operator $\widetilde{\mathcal{B}}_1$ is compact in $L^2(\Gamma)$. On the other hand, we can establish the following identity

$$\widetilde{\mathcal{B}}_2 := \frac{1}{2}I + K_L + \frac{\alpha_0}{2\alpha_1}I - 2\frac{\alpha_0}{\alpha_1}K_L^2 = -2\frac{\alpha_0}{\alpha_1}\left(\frac{1}{2}I + K_L\right)\left(-\frac{\alpha_0+\alpha_1}{2\alpha_0} + K_L\right)$$

and thus, the operator $\widetilde{\mathcal{B}}_2$ is the product of an operator that is Fredholm of index 0 and an invertible operator (indeed, since $\frac{\alpha_0+\alpha_1}{2\alpha_0} > \frac{1}{2}$, we can apply the results in Theorem 2.0.3), and hence, $\widetilde{\mathcal{B}}_2$ is itself Fredholm of index 0 in $L^2(\Gamma)$. Consequently, the operator $\mathcal{B}_1$ is a compact perturbation of a Fredholm operator of index 0 in $L^2(\Gamma)$. The conclusion of the Theorem follows once

$$w := DL_1\psi - 2\frac{\alpha_0}{\alpha_1}SL_1[N_{k_0+i\sigma_0}]\psi, \qquad \text{in } \mathbb{R}^2 \setminus \Gamma.$$

It follows that $\gamma_\Gamma^{D,ext} w = 0$ and hence $w = 0$ in Ω_0. Using relations (2.4) we derive

$$\gamma_\Gamma^{D,int} w = -\psi \qquad \gamma_\Gamma^{N,int} w = -2\frac{\alpha_0}{\alpha_1}N_{k_0+i\sigma_0}\psi.$$

Using Green's identities we obtain

$$\int_{\Omega_1}(|\nabla w|^2 - k_1^2 w)dx = 2\frac{\alpha_0}{\alpha_1}\int_\Gamma (N_{k_0+i\sigma_0}\psi)\ \overline{\psi}\ ds.$$

Using the fact that [4]

$$\Im \int_\Gamma (N_{k_0+i\sigma_0}\psi)\ \overline{\psi}\ ds > 0, \quad \psi \neq 0$$

we obtain that $\psi = 0$ which conclude the proof of the Theorem in the space $L^2(\Gamma) = H^0(\Gamma)$. Clearly, the arguments of the proof can be repeated verbatim in the Sobolev spaces $H^s(\Gamma)$ for all $s \in [-1, 0)$. The result in the remaining Sobolev spaces $H^s(\Gamma)$, $s \in (0, 1]$ follows then from duality arguments. ∎

Once the invertibility of the operator $\mathcal{B}_1$ was established, we immediately obtain a representation of the corresponding RtR operator

$$\mathcal{S}^1 = I - \alpha_1^{-1}(Z_0 + Z_1)\mathcal{B}_1^{-1}S_1. \tag{4.5}$$

The result establish in Theorem 4.0.1 remains valid in the case of impedance operators Z_1^a. Under increased regularity assumption on the curve Γ (e.g., Γ is C^3 or better), one can establish the compactness of the difference operator $N_{k_0+i\sigma_0} - PS(N_{k_0+i\sigma_0})$ [4], and the conclusion of Theorem 4.0.1 is true in the case of impedance operator Z_1^{PS}. Whether the aforementioned compactness property of the difference operator holds in the case of Lipschitz curves Γ is an open question. The arguments in the proof of Theorem 4.0.1 go through in the case of the exterior domain Ω_0 provided that k_0 is not an eigenvalue of the Laplacean with Ditichlet boundary conditions in the domain Ω_1. However, the well-posedness of the formulation in Theorem 4.0.1 cannot be establish for all positive wavenumbers k_0. We present in what follows a robust alternative BIE formulation [23] that can be shown to be well-posed for the same two choices of impedance operators Z_j and Z_j^a in Lipschitz domains. We start our presentation in the case of the bounded domain Ω_1, and we derive a system of BIE whose unknowns are the Cauchy data $(u_1|\Gamma, \partial_{n_1}u_1|_\Gamma)$. Applying the interior Dirichlet and Neumann traces to Green's identity in the domain Ω_1 we obtain

$$\begin{aligned} \left(\frac{1}{2}I + K_1\right) u_1|_\Gamma - S_1\partial_{n_1}u_1|_\Gamma &= 0 \\ -N_1 u_1|_\Gamma + \left(-\frac{1}{2}I + K_1^\top\right)\partial_{n_1}u_1|_\Gamma &= 0. \end{aligned}$$

Adding to the second equation above the impedance boundary condition we derive the following system of BIE

$$\begin{bmatrix} -\alpha_1^{-1}Z_1 + N_1 & -\frac{1}{2}I - K_1^\top \\ -\frac{1}{2}I - K_1 & S_1 \end{bmatrix} \begin{bmatrix} u_1|_\Gamma \\ \partial_{n_1}u_1|_\Gamma \end{bmatrix} = \begin{bmatrix} \varphi_1 \\ 0 \end{bmatrix}. \tag{4.6}$$

The well-posedness of the formulation (4.6) can be established by making use of the bilinear form

$$\langle (f,\varphi),(g,\psi)\rangle := \int_\Gamma fg + \int_\Gamma \varphi\psi, \quad (f,\varphi)\in H^{1/2}(\Gamma)\times H^{-1/2}(\Gamma),\ (g,\psi)\in H^{-1/2}(\Gamma)\times H^{1/2}(\Gamma).$$

Indeed, following the techniques in [23] we establish the following result:

Theorem 4.0.2 *The operator*

$$\mathcal{C}_1 := \begin{bmatrix} -\alpha_1^{-1}Z_1 + N_1 & -\frac{1}{2}I - K_1^\top \\ -\frac{1}{2}I - K_1 & S_1 \end{bmatrix}, \qquad \mathcal{C}_1 : H^{1/2}(\Gamma)\times H^{-1/2}(\Gamma) \to H^{-1/2}(\Gamma)\times H^{1/2}(\Gamma)$$

is invertible and its inverse is continuous.

Proof. We have that

$$\begin{aligned} \mathcal{C}_1 &= \mathcal{C}_{1,L} + \mathcal{C}_2 \\ \mathcal{C}_{1,L} &:= \begin{bmatrix} (2\frac{\alpha_0}{\alpha_1}+1)N_L & -\frac{1}{2}I - K_L^\top \\ -\frac{1}{2}I - K_L & S_L \end{bmatrix} \\ \mathcal{C}_2 &:= \begin{bmatrix} 2\alpha_0\alpha_1^{-1}(N_{k_0+i\sigma_0} - N_L) + (N_1 - N_L) & K_L^\top - K_1^\top \\ K_L - K_1 & S_1 - S_L \end{bmatrix}. \end{aligned}$$

Using the results in Theorem 2.0.2, we see that $\mathcal{C}_2 : H^{1/2}(\Gamma)\times H^{-1/2}(\Gamma) \to H^{-1/2}(\Gamma)\times H^{1/2}(\Gamma)$ is compact. In addition, we have that

$$\langle \mathcal{C}_{1,L}(f,\varphi),(f,\varphi)\rangle = (2\frac{\alpha_0}{\alpha_1}+1)\langle N_L f, f\rangle + \langle S_L\varphi,\varphi\rangle \geq c_1(2\frac{\alpha_0}{\alpha_1}+1)\|f\|^2_{H^{1/2}(\Gamma)} + c_2\|\varphi\|^2_{H^{-1/2}(\Gamma)}$$

which means that $\mathcal{C}_1$ satisfies a Gårding inequality. Thus, the result of the Theorem is completed once we establish the injectivity of the operator $\mathcal{C}_1$. Let $(f,\varphi)\in Ker(\mathcal{C}_1)$ and define

$$v_1 := DL_1 f - SL_1\varphi \qquad \text{in } \mathbb{R}^2\setminus\Gamma.$$

The fact that $(f, \varphi) \in Ker(\mathcal{C}_1)$ implies

$$\frac{1}{2} f + K_1 f - S_1 \varphi = 0 \qquad \text{on } \Gamma$$

which is to say that v_1 is a radiative solution of the Helmholtz equation in Ω_0 with zero Dirichlet boundary conditions on Γ. Hence, v_1 is identically zero in Ω_0. In particular, the exterior Neumann trace of v_1 is zero on Γ, which translates into

$$\frac{1}{2} \varphi - K_1^\top \varphi + N_1 f = 0 \qquad \text{on } \Gamma.$$

Again, $(f, \varphi) \in Ker(\mathcal{C}_1)$ also implies that

$$\frac{1}{2} \varphi + K_1^\top \varphi + \alpha_1^{-1} Z_0 f - N_1 f = 0 \qquad \text{on } \Gamma.$$

We obtain immediately from the last two identities that

$$\varphi = -\alpha_1^{-1} Z_1 f \qquad \text{on } \Gamma.$$

Using one more time the fact that v_1 is identically zero in Ω_0 we derive

$$\gamma_\Gamma^{D,int} v_1 = -f \qquad \gamma_\Gamma^{N,int} v_1 = -\varphi = 2 \frac{\alpha_0}{\alpha_1} N_{k_0 + i\sigma_0} f \qquad \text{on } \Gamma.$$

Using Green's identities we obtain

$$\int_{\Omega_1} (|\nabla v_1|^2 - k_1^2 v_1) dx = -2 \frac{\alpha_0}{\alpha_1} \int_\Gamma (N_{k_0 + i\sigma_0} f)\ \overline{f}\ ds.$$

Using the fact that [4]

$$\Im \int_\Gamma (N_{k_0 + i\sigma_0} f)\ \overline{f}\ ds > 0, \quad f \neq 0$$

we obtain that $f = 0$, and thus $\varphi = 0$, which concludes the proof of the Theorem.

■

The equivalent of formulation (4.6) cannot be shown to be well-posed in the case of the analogous impedance boundary value problem in the the exterior domain Ω_0, unless k_0 is not an eigenvalue of the Laplacean with Dirichlet boundary conditions in Ω_1. The remedy is to consider the following system of integral equations

$$\begin{bmatrix} -\alpha_0^{-1} Z_0 + N_0 & -\frac{1}{2} I - K_0^\top \\ \alpha_0^{-1} S_{k_0+i\sigma_0} Z_0 - \frac{1}{2} I - K_0 & S_0 + S_{k_0+i\sigma_0} \end{bmatrix} \begin{bmatrix} u_0|_\Gamma \\ \partial_{n_0} u_0|_\Gamma \end{bmatrix} = \begin{bmatrix} \varphi_0 \\ S_{k_0+i\sigma_0} \varphi_0 \end{bmatrix} \tag{4.7}$$

whose derivation is absolutely similar to that of equations (4.6) except that we add to both sides of the second equation in (4.6) the identity

$$\alpha_0^{-1} S_{k_0+i\sigma_0} Z_0 u_0 + S_{k_0+i\sigma_0} \partial_{n_0} u_0 = S_{k_0+i\sigma_0} \varphi_0.$$

We have

Theorem 4.0.3 *The operator*

$$\mathcal{C}_0 := \begin{bmatrix} -\alpha_0^{-1} Z_0 + N_0 & -\frac{1}{2} I - K_0^\top \\ \alpha_0^{-1} S_{k_0+i\sigma_0} Z_0 - \frac{1}{2} I - K_0 & S_0 + S_{k_0+i\sigma_0} \end{bmatrix}$$

with the mapping property $\mathcal{C}_0 : H^{1/2}(\Gamma) \times H^{-1/2}(\Gamma) \to H^{-1/2}(\Gamma) \times H^{1/2}(\Gamma)$ *is invertible with continuous inverse.*

Proof. Using similar arguments to those in the proof of Theorem 4.0.2, we can establish that the operator $\mathcal{C}_0$ is a compact perturbation of a sum of a coercive operator and an operator that is Fredholm of index 0. Thus, the result in the Theorem is complete once we establish the injectivity of the operator $\mathcal{C}_0$. Let $(f, \varphi) \in Ker(\mathcal{C}_0)$ and define

$$v_0 := -DL_0 f + SL_0 \varphi \qquad \text{in } \mathbb{R}^2 \setminus \Gamma.$$

Application of the Dirichlet trace corresponding to the interior domain Ω_1 to v_0 gives rise to the following identities

$$\gamma_\Gamma^{D,int} v_0 = -\frac{1}{2} f - K_0 f + S_0 \varphi$$

Given that $(f, \varphi) \in Ker(\mathcal{C}_0)$ implies that

$$\alpha_0^{-1} S_{k_0+i\sigma_0} Z_0 f - \frac{1}{2} f - K_0 f + S_0 \varphi + S_L \varphi = 0.$$

We obtain from the last two equations

$$\gamma_\Gamma^{D,int} v_0 + S_{k_0+i\sigma_0} \varphi + \alpha_0^{-1} S_{k_0+i\sigma_0} Z_0 f = 0. \tag{4.8}$$

Application of the Neumann trace corresponding to the interior domain Ω_1 to v_0 gives rise to the following identities

$$\gamma_\Gamma^{N,int} v_0 = N_0 f + \frac{1}{2} \varphi - K_0^\top \varphi.$$

Given that $(f, \varphi) \in Ker(\mathcal{C}_0)$ implies that

$$-\alpha_0^{-1} Z_0 f + N_0 f - \frac{1}{2} \varphi - K_0^\top \varphi = 0.$$

We obtain from the last two equations

$$\gamma_\Gamma^{N,int} v_0 - \varphi - \alpha_0^{-1} Z_0 f = 0 \tag{4.9}$$

and hence

$$S_{k_0+i\sigma_0} \gamma_\Gamma^{N,int} v_0 - S_{k_0+i\sigma_0} \varphi - \alpha_0^{-1} S_L Z_0 f = 0 \tag{4.10}$$

Combining equations (4.8) and (4.10) we get

$$S_{k_0+i\sigma_0} \gamma_\Gamma^{N,int} v_0 + \gamma_\Gamma^{D,int} v_0 = 0.$$

Using Green's identities we obtain

$$\int_{\Omega_1} (|\nabla v_0|^2 - k_0^2 v_0) dx = -2 \int_\Gamma (S_{k_0+i\sigma_0} \gamma_\Gamma^{N,int} v_0) \ \overline{\gamma_\Gamma^{N,int} v_0} \ ds.$$

Using the fact that [4]

$$\Im \int_\Gamma (S_{k_0+i\sigma_0} \psi) \ \overline{\psi} \ ds > 0, \quad \psi \neq 0$$

we obtain that $\gamma_\Gamma^{N,int} v_0 = 0$, and hence $\gamma_\Gamma^{D,int} v_0 = 0$, from which we conclude that v_0 is identically zero in Ω_1. Now using these newly found results in Equation (4.9) we get

$$\varphi = -\alpha_0^{-1} Z_0 f = 2 \frac{\alpha_0}{\alpha_1} N_{k_1+i\sigma_1} f.$$

On the other hand, we obtain that

$$\gamma_\Gamma^{D,ext} v_0 = f \qquad \gamma_\Gamma^{N,ext} v_0 = -\varphi.$$

We have that v_0 is a radiating solution of the Helmholtz equation in the domain Ω_0 satisfying

$$\Im \int_\Gamma \overline{\gamma_\Gamma^{D,ext} v_0} \ \gamma_\Gamma^{N,ext} v_0 \ ds = -2 \frac{\alpha_0}{\alpha_1} \int_\Gamma (N_{k_1+i\sigma_1} f) \ \overline{f} \ ds \leq 0$$

which implies that $v_0 = 0$ in Ω_0 [6], and thus $f = 0$ and $\varphi = 0$. ∎

Again, the results established in Theorem 4.0.2 and Theorem 4.0.3 can be replicated in the case of impedance operators $Z_j^a, j = 0, 1$. In case when the boundary Γ is more regular, then the compactness results about $N_{k_j+i\sigma_j} - PS(N_{k_j+i\sigma_j})$ can be invoked again to show robustness results similar to those in Theorem 4.0.2 and Theorem 4.0.3 for impedance operators $Z_j^{PS}, j = 0, 1$. We will discuss in the last Section the merits of each of the three formulations.

4.1 Well-posedness of the DDM Formulation

The well-posedness of the DDM formulation (3.5) in the space $L^2(\Gamma)$ (and all $H^s(\Gamma), s \in [-1, 1]$) hinges on the invertibility of the operator

$$I - \mathcal{S}^0\mathcal{S}^1 : L^2(\Gamma) \to L^2(\Gamma)$$

via the formula

$$(I + \mathcal{S})^{-1} = \begin{bmatrix} I + \mathcal{S}^1(I - \mathcal{S}^0\mathcal{S}^1)^{-1}\mathcal{S}^0 & -\mathcal{S}^1(I - \mathcal{S}^0\mathcal{S}^1)^{-1} \\ -(I - \mathcal{S}^0\mathcal{S}^1)^{-1}\mathcal{S}^0 & (I - \mathcal{S}^0\mathcal{S}^1)^{-1} \end{bmatrix}. \tag{4.11}$$

The invertibility of the operator $I - \mathcal{S}^0\mathcal{S}^1$, in turn, can be established *via* Fredholm arguments, at least in the case when Γ is C^3 or more regular. The key ingredient in our proof is the compactness of the double layer operators $K_L : L^2(\Gamma) \to L^2(\Gamma)$, which is valid under the additional regularity assumptions on the boundary Γ. We begin by establishing the following

Lemma 4.1.1 *The RtR operators $\mathcal{S}^j : L^2(\Gamma) \to L^2(\Gamma)$ corresponding to the impedance operators Z_j and Z_j^{PS}, $j = 0, 1$, are compact when the boundary Γ is C^3 or better.*

Proof. We start from formula (4.5) and we get

$$\begin{aligned}
\mathcal{S}^1 &= I - \alpha_1^{-1}(Z_0 + Z_1)\mathcal{B}_1^{-1}S_1 = (Z_0 + Z_1)\mathcal{B}_1^{-1}\mathcal{B}_1^1(Z_0 + Z_1)^{-1} \\
\mathcal{B}_1^1 &:= \mathcal{B}_1 - \alpha_1^{-1}S_1(Z_0 + Z_1) = \mathcal{B}_1 + 2\alpha_1^{-1}S_1(\alpha_1 N_{k1+i\sigma_1} + \alpha_0 N_{k_0+i\sigma_0}) \\
&= \mathcal{B}_1 - \frac{1}{2}\alpha_1^{-1}(\alpha_0 + \alpha_1)I + 2\alpha_1^{-1}(\alpha_0 + \alpha_1)K_L^2 + \mathcal{B}_1^2 \\
\mathcal{B}_1^2 &:= 2\alpha_1^{-1}(\alpha_0 + \alpha_1)(S_1 - S_L)N_L + 2\alpha_1^{-1}S_1(\alpha_1(N_{k1+i\sigma_1} - N_L) + \alpha_0(N_{k_0+i\sigma_0} - N_L)).
\end{aligned}$$

We recall from the proof of Theorem 4.0.1 that the operator $\mathcal{B}_1$ was expressed in the form

$$\mathcal{B}_1 = \frac{1}{2}\alpha_1^{-1}(\alpha_0 + \alpha_1)I + K_L - 2\frac{\alpha_0}{\alpha_1}K_L^2 + \widetilde{\mathcal{B}}_1$$

where the operator $\widetilde{\mathcal{B}_1} : L^2(\Gamma) \to L^2(\Gamma)$ is compact. Putting together these two representations we obtain

$$\mathcal{B}_1^1 = K_L + 2K_L^2 + \mathcal{B}_1^2 + \widetilde{\mathcal{B}}_1.$$

Using the mapping properties recounted in Theorem 2.0.2, we see immediately that $\mathcal{B}_1^2 : L^2(\Gamma) \to L^2(\Gamma)$ is also compact. We note that thus far we used only the fact that Γ is Lipschitz. In case when Γ is C^3 or better, $K_L : L^2(\Gamma) \to L^2(\Gamma)$ is itself a compact operator, and thus $\mathcal{B}_1^1 : L^2(\Gamma) \to L^2(\Gamma)$ is compact. Now

$$\mathcal{S}^1 = (Z_0 + Z_1)\mathcal{B}_1^{-1}\mathcal{B}_1^1(Z_0 + Z_1)^{-1}$$

can be seen to be compact in $L^2(\Gamma)$ if we use the compactness of $\mathcal{B}_1^1$ and the mapping properties of the operators involved in the representation of $\mathcal{S}^1$ above. A similar argument can be aplied in the case of the RtR operator $\mathcal{S}^0$ when k_0 is not an eigenvalue of the Dirichlet Laplacean in the domain Ω_1. The same procedure can be applied in the case of the representation of the RtR operators *via* the operators $\mathcal{A}_j, j = 0, 1$ defined in Equation (4.3), which is robust for both domains Ω_j and all positive wavenumbers k_j with $j = 0, 1$. Indeed, we obtain

$$\mathcal{S}^j = (Z_0 + Z_1)\mathcal{A}_j^{-1}\mathcal{A}_j^1(Z_0 + Z_1)^{-1},\ j = 0, 1$$

where it can be shown using formula (4.2) that

$$\mathcal{A}_j^1 = 2K_L + 2K_L^2 - 4K_L^3 + \mathcal{A}_j^2,\ j = 0, 1$$

with $\mathcal{A}_j^2 : L^2(\Gamma) \to L^2(\Gamma)$ compact when Γ is Lipschitz. Clearly, the assumption that Γ is C^3 implies that both operators $\mathcal{A}_j^1 : L^2(\Gamma) \to L^2(\Gamma)$ are compact and thus both RtR operators $\mathcal{S}^j : L^2(\Gamma) \to L^2(\Gamma)$ are compact. Under the regularity assumption of the interface Γ, the arguments in the proof of the Lemma carry over in the case of RtR operators corresponding to the impedance operators $Z_j^{PS}, j = 0, 1$. ∎

Remark 4.1.2 *In the Lipschitz case, one can show that*

$$I - \mathcal{S}^0\mathcal{S}^1 = (Z_0 + Z_1)\mathcal{B}_0^{-1}(\mathcal{B}_0\mathcal{B}_1 - \mathcal{B}_0^1\mathcal{B}_1^1)\mathcal{B}_1^{-1}(Z_0 + Z_1)^{-1} + \mathcal{S}_R$$

where $\mathcal{S}_R : L^2(\Gamma) \to L^2(\Gamma)$ *is compact. A simple calculation delivers*

$$\mathcal{B}_0\mathcal{B}_1 - \mathcal{B}_0^1\mathcal{B}_1^1 = \frac{2(\alpha_0 + \alpha_1)^2}{\alpha_0\alpha_1}\left(\frac{1}{2}I + K_L\right)^2\left(\frac{1}{2}I - K_L\right).$$

Given that $\frac{1}{2}I + K_L$ *is invertible in* $L^2(\Gamma)$ *and* $\frac{1}{2}I - K_L$ *is Fredholm of index zero in* $L^2(\Gamma)$*, it follows that* $I - \mathcal{S}^0\mathcal{S}^1$ *is also Fredholm of index zero in* $L^2(\Gamma)$*.*

We are now in the position to prove the main result

Theorem 4.1.3 *The DDM operators* $I - \mathcal{S}^0\mathcal{S}^1 : L^2(\Gamma) \to L^2(\Gamma)$ *corresponding to the impedance operators* Z_j *and* Z_j^{PS}*,* $j = 0, 1$*, is invertible with continous inverse when the boundary* Γ *is* C^3 *or better.*

Proof. Given the result in Lemma 4.1.1, it suffices to establish the injenctivity of the DDM operator $I - \mathcal{S}^0\mathcal{S}^1$. Let $\varphi \in Ker(I - \mathcal{S}^0\mathcal{S}^1)$. Consider the following Helmholtz equation

$$\begin{aligned} \Delta w_1 + k_1^2 w_1 &= 0 \qquad \text{in } \Omega_1 \\ \partial_{n_1} w_1 + \alpha_1^{-1} Z_1 w_1 &= \varphi \qquad \text{on } \Gamma. \end{aligned}$$

Then, we have that

$$\mathcal{S}^1\varphi = \partial_{n_1} w_1 - \alpha_1^{-1} Z_0 w_1.$$

Consider also the following Helmholtz equation

$$\begin{aligned} \Delta w_0 + k_0^2 w_0 &= 0 \qquad \text{in } \Omega_0 \\ \partial_{n_0} w_0 + \alpha_0^{-1} Z_0 w_0 &= \mathcal{S}^1\varphi \qquad \text{on } \Gamma. \end{aligned}$$

and w_0 radiative at infinity. We have then

$$\mathcal{S}^0\mathcal{S}^1\varphi = \partial_{n_0} w_0 - \alpha_0^{-1} Z_1 w_0 = \partial_{n_1} w_1 + \alpha_1^{-1} Z_1 w_1$$

using the fact that $\mathcal{S}^0\mathcal{S}^1\varphi = \varphi$. Thus, we have derived the following system of equation on Γ

$$\begin{aligned} \partial_{n_0} w_0 - \alpha_0^{-1} Z_1 w_0 &= \partial_{n_1} w_1 + \alpha_1^{-1} Z_1 w_1 \\ \partial_{n_0} w_0 + \alpha_0^{-1} Z_0 w_0 &= \partial_{n_1} w_1 - \alpha_1^{-1} Z_0 w_1. \end{aligned}$$

from which we get that

$$(Z_0 + Z_1)(\alpha_0^{-1} w_0 + \alpha_1^{-1} w_1) = 0 \qquad \text{on } \Gamma.$$

Given the invertibility of the operator $Z_0 + Z_1$ we obtain

$$w_0|_\Gamma = -\alpha_1^{-1}\alpha_0 w_1|_\Gamma$$

and then

$$\partial_{n_1} w_0|_\Gamma = -\partial_{n_1} w_1|_\Gamma.$$

Using the last two identities we derive

$$\Im \int_\Gamma \overline{\partial_{n_1} w_0}\ w_0\ ds = \alpha_1^{-1}\alpha_0 \Im \int_\Gamma \overline{\partial_{n_1} w_1}\ w_1\ ds = \alpha_1^{-1}\alpha_0 \Im \int_{\Omega_1} (|\nabla w_1|^2 - k_1^2 w_1) dx = 0.$$

The last relation implies that $w_0 = 0$ identically in Ω_0, from which follows immediately that $w_1 = 0$ in Ω_1, and hence $\varphi = 0$. ∎

We turn next to the case of DDM formulations with impedance operators $Z_j^a, j = 0, 1$. The situation is quite different in this case due to the entirely different mapping properties of the operators $Z_j^a, j = 0, 1$. We show the following result:

Theorem 4.1.4 *The DDM operators* $I - \mathcal{S}^0\mathcal{S}^1 : L^2(\Gamma) \to H^1(\Gamma)$ *corresponding to the impedance operators* Z_j^a, $j = 0, 1$, *are invertible with continous inverse when the boundary* Γ *is* C^3 *or better.*

Proof. We note that is suffices to establish the Fredholmness of the operators $I - \mathcal{S}^0\mathcal{S}^1 : L^2(\Gamma) \to H^1(\Gamma)$. The key ingredient is the result established in formula (4.2), which in the case when the boundary Γ is C^3 or better simply implies that

$$\mathcal{A}_j = \alpha_j^{-1}(\alpha_0 + \alpha_1)I + \mathcal{A}_j^1, j = 0, 1$$

where the operators $\mathcal{A}_j : L^2(\Gamma) \to H^1(\Gamma)$, and thus $\mathcal{A}_j : L^2(\Gamma) \to L^2(\Gamma)$ are compact for $j = 0, 1$. In the light of this fact, we obatin from formula (4.3)

$$\mathcal{S}^j = I - 2(\alpha_0 + \alpha_1)^{-1}(Z_0^a + Z_1^a)S_L + \widetilde{\mathcal{S}}^j, \ j = 0, 1$$

where $\widetilde{\mathcal{S}}^j : L^2(\Gamma) \to L^2(\Gamma)$ are compact for $j = 0, 1$. Clearly, we have that

$$I - \mathcal{S}^0\mathcal{S}^1 = 4(\alpha_0 + \alpha_1)^{-1}(Z_0^a + Z_1^a)S_L + \mathcal{D},$$

where $\mathcal{D} : L^2(\Gamma) \to L^2(\Gamma)$ is compact. Clearly, since $\Re(Z_j^a) > 0, \ j = 0, 1$, the operator $I - \mathcal{S}^0\mathcal{S}^1$ satisfy a Gårding inequality given that $\Re \int_\Gamma S_L\varphi \ \overline{\varphi} \ ds \geq c\|\varphi\|^2$, and thus the operator $I - \mathcal{S}^0\mathcal{S}^1 : L^2(\Gamma) \to H^1(\Gamma)$ is Fredholm of index zero. Its injectivity can be established by the same arguments as in the proof of Theorem 4.1.3. ∎

CHAPTER 5

HELMHOLTZ TRANSMISSION PROBLEMS IN COMPOSITE DOMAINS

We consider the problem of time-harmonic fields scattering by scattering structures which occupy a bounded region and feature multiple junctions which are points where more than three interfaces of material discontinuity meet (e.g., the case in Figure 5.1). For simplicity, we focus our treatment of transmission problems with multiple junction domains on the two subdomain case depicted in Figure 5.1. Specifically, we seek to solve the scattering problem that consists of finding the fields u_0, u_1, and u_2 as solutions of the system of equations

$$\begin{aligned} \Delta u_j + k_j^2 u_j &= 0 \qquad \text{in } \Omega_j \\ u_j + \delta_j^0 u^{inc} &= u_\ell + \delta_\ell^0 u^{inc} \qquad \text{on } \Gamma_{j\ell} = \partial\Omega_j \cap \partial\Omega_\ell \\ \partial_{n_j} u_j + \delta_j^0 \partial_{n_j} u^{inc} &= -(\partial_{n_\ell} u_\ell + \delta_\ell^0 \partial_{n_\ell} u^{inc}) \qquad \text{on } \Gamma_{j\ell} \\ \lim_{r\to\infty} r^{1/2}(\partial u_0/\partial r - ik_0 u_0) &= 0, \end{aligned} \tag{5.1}$$

where δ_j^0 and δ_ℓ^0 stand for Kronecker operators, that is δ_j^0 is the identity operator if $j = 0$ and the null operator otherwise. Here, the incident field u^{inc} is assumed to satisfy the Helmholtz equation with wavenumber k_0 in the unbounded domain Ω_0, and the wavenubers k_j are defined as $k_j = \omega\sqrt{\varepsilon_j}$. We denoted by n_j the unit normal on the boundary $\partial\Omega_j$ pointing to the exterior of the domain Ω_j. We assume in what follows that ε_j are all real numbers, extensions to more general cases being straightforward. The well posedness of the transmission problem was established in [15].

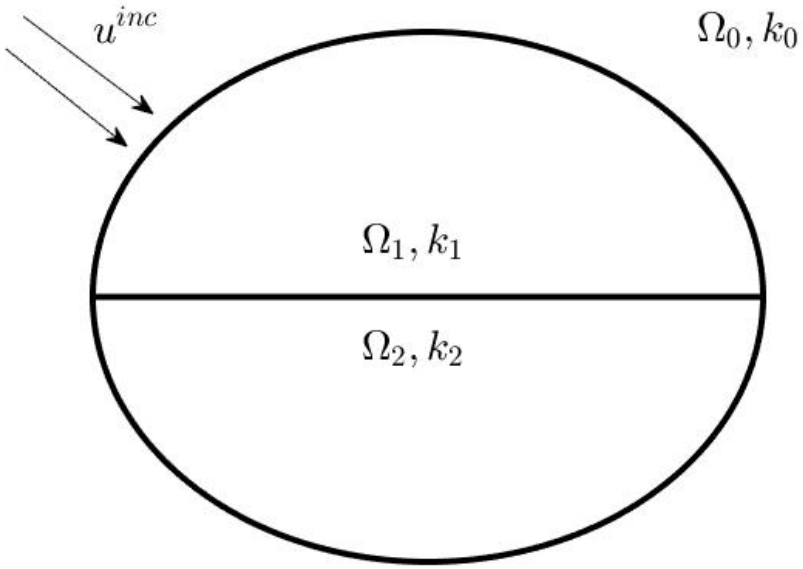

Figure 5.1 Typical triple junction configuration.

In what follows, we review two main formulations of the transmission problem 5.1. One relies on boundary integral equations, and the other is a Domain Decomposition Method.

CHAPTER 6

MULTI-TRACE FORMULATIONS(HIPTMAIR JEREZ-HANCKES)

6.1 The Case of One Domain

In this part, we will derive the multi-trace formulations for the one interior domain Ω_1 case. By Green's identities, we write the wave solution in the form of a combined acoustic double- and single-layer potential:

$$\begin{aligned} u_0 &= DL_0\gamma_D^0 u_0 - SL_0\gamma_N^0 u_0 \qquad in \quad \Omega_0 \\ u_1 &= SL_1\gamma_N^0 u_1 - DL_1\gamma_D^0 u_1 \qquad in \quad \Omega_1 \end{aligned} \tag{6.1}$$

Then, from boundary conditions, we get

$$K_0\gamma_D^0 u_0 - S_0\gamma_N^0 u_0 = \frac{1}{2}\gamma_D^0 u_0 = \frac{1}{2}\gamma_D^0 u_1 - \frac{1}{2}\gamma_D^0 u^{inc}$$

So

$$K_0\gamma_D^0 u_0 - S_0\gamma_N^0 u_0 - \frac{1}{2}\gamma_D^0 u_1 = -\frac{1}{2}\gamma_D^0 u^{inc}$$

Similarity,

$$\begin{aligned} N_0\gamma_D^0 u_0 - K_0^T\gamma_N^0 u_0 - \frac{1}{2}\gamma_N^0 u_1 &= -\frac{1}{2}\gamma_N^0 u^{inc} \\ S_1\gamma_N^0 u_1 - K_1\gamma_N^0 u_1 - \frac{1}{2}\gamma_D^0 u_0 &= \frac{1}{2}\gamma_D u^{inc} \\ K_1^T\gamma_N^0 u_1 - N_1\gamma_N^0 u_1 - \frac{1}{2}\gamma_N^0 u_0 &= \frac{1}{2}\gamma_N u^{inc} \end{aligned} \tag{6.2}$$

Finally, we get the following 4×4 linear system

$$\begin{bmatrix} K_0 & -S_0 & -\frac{Id}{2} & 0 \\ N_0 & -K_0^T & 0 & -\frac{Id}{2} \\ -\frac{Id}{2} & 0 & -K_1 & S_1 \\ 0 & -\frac{Id}{2} & -N_1 & K_1^T \end{bmatrix} \begin{bmatrix} \gamma_D^0 u_0 \\ \gamma_N^0 u_0 \\ \gamma_D^1 u_1 \\ \gamma_N^1 u_1 \end{bmatrix} = -\frac{1}{2} \begin{bmatrix} \gamma_D^0 u^{inc} \\ \gamma_N^0 u^{inc} \\ -\gamma_D^0 u^{inc} \\ -\gamma_N^0 u^{inc} \end{bmatrix} (MTF).$$

The multi-trace terminology is owed to the fact that the unknowns in this formulation are the interior/exterior Dirichlet and Neumann traces on the interface of material discontinuity. If we denote by

$$\mathcal{A}_0 := \begin{bmatrix} K_0 & -S_0 \\ N_0 & -K_0^T \end{bmatrix}$$

$$\mathcal{A}_1 := \begin{bmatrix} -K_1 & S_1 \\ -N_1 & K_1^T \end{bmatrix}$$

and

$$Id_2 := \begin{bmatrix} I & 0 \\ 0 & I \end{bmatrix}.$$

then it follows from Calderon identities that

$$\mathcal{A}_0^2 = \frac{Id_2}{4}.$$

$$\mathcal{A}_1^2 = \frac{Id_2}{4}.$$

This very simple fact allows us to eliminate *via* Schur complements the unknown pair $(\gamma_D^0 u_0, \gamma_N^0 u_0)^\top$ from the MTF system. Indeed, we get that

$$\begin{bmatrix} \gamma_D^0 u_0 \\ \gamma_N^0 u_0 \end{bmatrix} = -2\mathcal{A}_0 \begin{bmatrix} \gamma_D^0 u^{inc} \\ \gamma_N^0 u^{inc} \end{bmatrix} + 2\mathcal{A}_0 \begin{bmatrix} \gamma_D^0 u_1 \\ \gamma_N^0 u_1 \end{bmatrix},$$

which if we plug in the last two equations in the MTF, we get

$$\begin{bmatrix} -(K_0 + K_1) & S_0 + S_1 \\ -(N_0 + N_1) & K_0^T + K_1^T \end{bmatrix} \begin{bmatrix} \gamma_D^0 u_1 \\ \gamma_N^0 u_1 \end{bmatrix} = \begin{bmatrix} \gamma_D^0 u^{inc} \\ \gamma_N^0 u^{inc} \end{bmatrix}, \tag{6.3}$$

if we take into account Green's identities applied to the incident field. The formulation in Equation (6.3) is the formulation of the first kind introduced by Costabel-Stephan [7].

One the other side, we write

$$\gamma_c u_0 = \begin{bmatrix} \gamma_D^0 u_0 \\ \gamma_N^0 u_0 \end{bmatrix}$$

and

$$\gamma_c u_1 = \begin{bmatrix} \gamma_D^0 u_1 \\ \gamma_N^0 u_1 \end{bmatrix}$$

By property of $\mathcal{A}_0$ and $\mathcal{A}_1$, we get preconditioners of MTF1,

$$\begin{bmatrix} \mathcal{A}_0 & -\frac{Id_2}{2} \\ -\frac{Id_2}{2} & \mathcal{A}_0 \end{bmatrix}^2 \begin{bmatrix} \gamma_c u_0 \\ \gamma_c u_1 \end{bmatrix} = \begin{bmatrix} \mathcal{A}_0 & -\frac{Id_2}{2} \\ -\frac{Id_2}{2} & \mathcal{A}_0 \end{bmatrix} \begin{bmatrix} \gamma_c u^{inc} \\ \gamma_c u^{inc} \end{bmatrix}$$

which equals

$$\begin{bmatrix} \frac{Id_2}{4} & -\frac{1}{2}(\mathcal{A}_0 + \mathcal{A}_1) \\ -\frac{1}{2}(\mathcal{A}_0 + \mathcal{A}_1) & \frac{Id_2}{4} \end{bmatrix} \begin{bmatrix} \gamma_c u_0 \\ \gamma_c u_1 \end{bmatrix} = \begin{bmatrix} \mathcal{A}_0 & -\frac{Id_2}{2} \\ -\frac{Id_2}{2} & \mathcal{A}_0 \end{bmatrix} \begin{bmatrix} \gamma_c u^{inc} \\ \gamma_c u^{inc} \end{bmatrix}$$

Notice that

$$(\mathcal{A}_0 + \mathcal{A}_1) = \begin{bmatrix} K_0 - K_1 & S_1 - S_0 \\ N_0 - N_1 & K_1^T - K_0^T \end{bmatrix}$$

is a compact operater.

6.2 The Case of Two Subdomains

We move on to transmission problem for two domains with MTF method. By Green's identities:

$$\begin{aligned} u^s &= DL_0\gamma_D^0 u_0 - SL_0\gamma_N^0 u_0 \qquad in \quad \Omega_0 \\ u_1 &= SL_0\gamma_N^0 u_1 - DL_0\gamma_D^0 u_1 \qquad in \quad \Omega_1 \\ u_2 &= SL_0\gamma_N^0 u_2 - DL_0\gamma_D^0 u_2 \qquad in \quad \Omega_2 \end{aligned} \tag{6.4}$$

We use $\Gamma_{10} = \partial\Omega_1 \setminus \partial\Omega_0$, $\Gamma_{00} = \partial\Omega_1 \cup \partial\Omega_2$, $\Gamma_{20} = \partial\Omega_2 \setminus \partial\Omega_1$, $\Gamma_{12} = \partial\Omega_1 \cap \partial\Omega_0$. And then define extensions by zero operaters and restriction operators. For instance, $R_{ij}\varphi_j$denotes the restriction of a functionφ_j defined on $\partial\Omega_j$to $\partial\Omega_i \cap \partial\Omega_j$ and $E_{ij}^i\varphi_{ij} = \begin{cases} \varphi_{ij} \quad on \quad \partial\Omega_i \cap \partial\Omega_j \\ 0 \quad on \quad \partial\Omega_i \setminus \partial\Omega_j \end{cases}$, where φ_{ij} is a function defined on $\partial\Omega_i \setminus \partial\Omega_j$. From Equation (6.4), we obtain

$$\begin{aligned} \frac{1}{2}\gamma_D^0 u_0 &= K_0\gamma_D^0 u_0 - S_0\gamma_N^0 u_0 \qquad on \quad \partial\Omega_0 \\ \frac{1}{2}\gamma_N^0 u_0 &= N_0\gamma_D^0 u_0 - K_0^T\gamma_N^0 u_0 \qquad on \quad \partial\Omega_0 \end{aligned} \tag{6.5}$$

$$\begin{aligned} \frac{1}{2}\gamma_D^j u_j &= S_j\gamma_N^0 u_j - K_j\gamma_D^0 u_j \qquad on \quad \partial\Omega_j \qquad j = 1,2 \\ \frac{1}{2}\gamma_N^j u_j &= K_j^T\gamma_N^0 u_j - N_j\gamma_D^0 u_j \qquad on \quad \partial\Omega_j \qquad j = 1,2 \end{aligned} \tag{6.6}$$

For the first equation of (6.5), we consider$\gamma_D^0 u_0$ on different parts of Ω_0

$$\begin{aligned} &(1) \qquad \gamma_D^0 u_0 = -\gamma_D^0 u^{inc}|_{\Gamma_{10}} + R_{01}\gamma_D^1 u_1 \qquad on \quad \Gamma_{10} \\ &(2) \qquad \gamma_D^0 u_0 = -\gamma_D^0 u^{inc}|_{\Gamma_{10}} + R_{02}\gamma_D^2 u_2 \qquad on \quad \Gamma_{20} \end{aligned}$$

combine (1) and (2) as

$$\gamma_D^0 u_0 = -\gamma_D^0 u^{inc} + E_{10}^0 R_{01}\gamma_D^1 u_1 + E_{20}^0 R_{02}\gamma_D^2 u_2 \qquad on \quad \Omega_0$$

Similarly, we can get

$$\gamma_N^0 u_0 = -\gamma_N^0 u^{inc} + E_{10}^0 R_{01} \gamma_N^1 u_1 + E_{20}^0 R_{02} \gamma_N^2 u_2 \qquad on \quad \Omega_0$$

Let us define $X_{01} = E_{10}^0 R_{01}$,$X_{02} = E_{20}^0 R_{02}$ to get a simple form .

$$\begin{aligned} \gamma_D^0 u_0 &= -\gamma_D^0 u^{inc} + X_{01} \gamma_D^1 u_1 + X_{02} \gamma_D^2 u_2 \qquad on \quad \Omega_0 \\ \gamma_N^0 u_0 &= -\gamma_N^0 u^{inc} + X_{01} \gamma_N^1 u_1 + X_{02} \gamma_N^2 u_2 \qquad on \quad \Omega_0 \end{aligned} \tag{6.7}$$

Now from the first equation of (6.6)

$$S_1 \gamma_N^1 u_1 - K_1 \gamma_D^0 u_1 - \frac{1}{2} \gamma_D^1 u_1 = 0 \qquad on \quad \partial\Omega_1$$

then consider it on different part of boundary

$$\begin{aligned} \gamma_D^1 u_1 &= \gamma_D^0 u^{inc}|_{\Gamma_{10}} + R_{10} \gamma_D^0 u_0 \qquad on \quad \Gamma_{10} \\ \gamma_D^1 u_1 &= R_{12} \gamma_D^2 u_2 \qquad on \quad \Gamma_{12} \end{aligned}$$

combine them together

$$\gamma_D^1 u_1 = E_{10}^1 R_{10} \gamma_D^0 u^{inc} + E_{10}^1 R_{10} \gamma_D^0 u_0 + E_{12}^1 R_{12} \gamma_D^2 u_2 \qquad on \quad \Omega_1$$

Similarly, we can get

$$\gamma_N^1 u_1 = E_{10}^1 R_{10} \gamma_N^0 u^{inc} + E_{10}^1 R_{10} \gamma_N^0 u_0 - E_{12}^1 R_{12} \gamma_N^2 u_2 \qquad on \quad \Omega_1$$

Let us define $X_{10} = E_{10}^1 R_{10}$, and $X_{12} = E_{12}^1 R_{12}$ and we express the continuity conditions of the Dirichlet and Neumann traces on $\partial\Omega_1$ in the form

$$\begin{aligned} \gamma_D^1 u_1 &= X_{10} \gamma_D^0 u^{inc} + X_{10} \gamma_D^0 u_0 + X_{12} \gamma_D^2 u_2 \qquad on \quad \partial\Omega_1 \\ \gamma_N^1 u_1 &= -X_{10} \gamma_N^0 u^{inc} - X_{10} \gamma_N^0 u_0 - X_{12} \gamma_N^2 u_2 \qquad on \quad \partial\Omega_1 \end{aligned} \tag{6.8}$$

By the same method, we can get formulations for $\gamma_D^2 u_2$ and $\gamma_N^2 u_2$. At last, we get a linear system which is referred to as the Multi-Trace Formulation

$$\begin{bmatrix} K_0 & -S_0 & -\frac{1}{2}X_{01} & 0 & \frac{1}{2}X_{02} & 0 \\ N_0 & -K_0^\top & 0 & -\frac{1}{2}X_{01} & 0 & -\frac{1}{2}X_{02} \\ \frac{1}{2}X_{10} & 0 & K_1 & -S_1 & \frac{1}{2}X_{12} & 0 \\ 0 & -\frac{1}{2}X_{10} & N_1 & -K_1^\top & 0 & -\frac{1}{2}X_{12} \\ \frac{1}{2}X_{20} & 0 & \frac{1}{2}X_{21} & 0 & K_2 & -S_2 \\ 0 & -\frac{1}{2}X_{20} & 0 & -\frac{1}{2}X_{21} & N_2 & -K_2^\top \end{bmatrix} \begin{bmatrix} \gamma_D^0 u_0 \\ \gamma_N^0 u_0 \\ \gamma_D^1 u_1 \\ \gamma_N^1 u_1 \\ \gamma_D^2 u_2 \\ \gamma_N^2 u_2 \end{bmatrix} = \frac{1}{2} \begin{bmatrix} \gamma_D^0 u^{inc} \\ \gamma_N^0 u^{inc} \\ -X_{10}\gamma_D^0 u^{inc} \\ X_{10}\gamma_N^0 u^{inc} \\ -X_{20}\gamma_D^0 u^{inc} \\ X_{20}\gamma_N^0 u^{inc} \end{bmatrix} \quad (MTF2).$$

The well-posedness of the MTF2 system in the space $(\gamma_D^j u_j, \gamma_N^j u_j) \in H^{1/2}(\partial\Omega_j) \times H^{-1/2}(\partial\Omega_j), j = 0, 1, 2$ was established in the literature.

CHAPTER 7

DOMAIN DECOMPOSITION METHOD

7.1 Domain Decomposition Method

Domain Decomposition Methods are natural candidates for numerical solution of transmission problems (5.1). A non-overlapping Domain Decomposition (DD) approach for the solution of Equation (5.1) consists of solving subdomain problems with matching Robin boundary conditions on the common subdomain interfaces [8]. Indeed, this procedure amounts to computing the subdomain solutions

$$\begin{aligned} \Delta u_j + k_j^2 u_j &= 0 \qquad \text{in } \Omega_j \\ (\partial_{n_j} u_j + \delta_j^0 \partial_{n_j} u^{inc}) + i\eta(u_j + \delta_j^0 u^{inc}) &= -(\partial_{n_\ell} u_\ell + \delta_\ell^0 \partial_{n_\ell} u^{inc} + i\eta(u_\ell + \delta_\ell^0 u^{inc}) \qquad \text{on } \Gamma_{j\ell}. \end{aligned} \tag{7.1}$$

In Equation (7.1) η is assumed to be a positive number. The latter requirement is needed to ensure the well posedness of the impedance boundary value Helmholtz problem in the exterior domain Ω_0 [6]. In all the numerical examples in this text we took $\eta = k_0$.

In order to describe the DD method more concisely we introduce subdomain Robin-to-Robin (RtR) maps [14]. Given a subdomain Ω_j we define the RtR map $\mathcal{S}^j$ in the following manner:

$$\mathcal{S}^j(\psi_j) := (\partial_{n_j} u_j - i\eta\, u_j)|_{\partial\Omega_j} \tag{7.2}$$

where u_j is the solution of the following problem:

$$\begin{aligned} \Delta u_j + k_j^2 u_j &= 0 \text{ in } \Omega_j \\ \partial_{n_j} u_j + i\eta u_j &= \psi_j \text{ on } \partial\Omega_j. \end{aligned}$$

In the case when Ω_j is the exterior domain Ω_0, we further require in the definition of the RtR map $\mathcal{S}^0$ that u_0 is radiative at infinity. The DD method computes the global

Robin data

$$f = \{f_j := (\partial_{n_j} u_j + i\eta\ u_j)|_{\partial\Omega_j},\ 0 \le j \le 2\}$$

as the solution of the following linear system that incorporates the subdomain RtR maps $\mathcal{S}^j, j = 0, 1, 2$ previously defined

$$(I + A)f = g, \quad A = \Pi\mathcal{S}, \quad \mathcal{S} = \begin{bmatrix} \mathcal{S}^1 & 0 & 0 \\ 0 & \mathcal{S}^2 & 0 \\ 0 & 0 & \mathcal{S}^0 \end{bmatrix}, \quad \Pi = \begin{bmatrix} 0 & \Pi_{12} & \Pi_{10} \\ \Pi_{21} & 0 & \Pi_{20} \\ \Pi_{01} & \Pi_{02} & 0 \end{bmatrix}. \tag{7.3}$$

In Equation (7.3) we denoted $f = [f_1\ f_2\ f_0]^\top$ and

$$\begin{aligned} g &= [g_1\ g_2\ g_0]^\top, \\ g_1 &= X_{01}(-\partial_{n_0} u^{inc} + i\eta u^{inc})|_{\partial\Omega_0} \\ g_2 &= X_{02}(-\partial_{n_0} u^{inc} + i\eta u^{inc})|_{\partial\Omega_0} \\ g_0 &= (-\partial_{n_0} u^{inc} - i\eta u^{inc})|_{\partial\Omega_0}. \end{aligned} \tag{7.4}$$

Remark 7.1.1 *The domains $\Omega_j,\ 1 \le j$ can be further subdivided into smaller subdomains, in which case the DD system* (7.3) *has to be augmented to incorporate the additional Robin data on the new interfaces. The size of the subdomains (in terms of wavelengths) should ideally be such that the computation/application of the corresponding RtR operators can be performed efficiently.*

We note that the matrix A in Equation (7.3) is not stored in practice, and, due to its possibly large size, the DD linear system (7.3) is typically solved in practice *via* iterative methods. Iterative solvers (e.g., Jacobi, GMRES) for the solution of DD linear systems of the type described in Equation (7.3) require large numbers of iterations, especially in the case of larger numbers of subdomains. This shortcoming can be attributed to the choice of Robin boundary conditions and the outflow/inflow of information from a subdomain to its neighboring subdomains associated with it. Ideally the subdomain boundary conditions have to be chosen

so that information flows out of the subdomain and no information is reflected back into the subdomain. This can be achieved if the term $i\eta$ in Equation (7.3) is replaced by the adjacent subdomain Dirichlet to Neumann (DtN) operator restricted to the common interface—in this way the Jacobi scheme converges in precisely two iterations [22]. Since DtN maps are not always well defined and expensive to compute even when properly defined, easily computable approximations of DtN maps can be employed effectively to lead to faster convergence rates of GMRES solvers for DDM algorithms [3], at least in the case where the subdomain interfaces do not coincide with those of material discontinuity. In order to get a better insight on the properties of DDM with various transmission conditions, we turn our attention in the future part to the one dimensional case, whereby all calculations are exact.

We describe in what follows the main ideas behind using DtN maps in a DD algorithm.

7.2 DDM with Generalized Robin Boundary Conditions

The rate of the convergence of iterative Krylov subspace solvers of the DDM linear system (7.3) is largely determined by the choice of the Robin boundary conditions therein. More effective Robin/impedance boundary conditions on the subdomain interfaces are known to improve the performance of iterative DDM solvers [23, 3, 27, 13]. These generalized Robin boundary conditions consist of replacing the classical $i\eta$ term by operators that approximate the Dirichlet-to-Neumann (DtN) operators of adjacent domains. For instance, it can be easily shown that the ideal Robin operator on the interface Γ_{12} corresponding to the domain Ω_1 consists of the operator $Y^2|_{\Gamma_{21}}$, where Y^2 is the DtN operator corresponding to the domain Ω_2 with zero Dirichlet boundary conditions on $\partial\Omega_2 \setminus \Gamma_{21}$. With this very choice, the ensuing DDM algorithm converges in precisely two iterations [22], at least in the case when Ω_j are half planes. Similarly, the ideal Robin operator on the interface Γ_{10} corresponding to the

domain Ω_1 can be shown to consist of the operator $Y^0|_{\Gamma_{01}}$. However, DtN operators are not always defined for interior subdomains (they are always well defined in the exterior domain Ω_0), and even when properly defined, DtN are non-local operators whose computation can be expensive. Their computation, whenever possible, can be obtained via boundary integral operators. For instance, using Green's identities in the domain Ω_2 and taking into consideration the null Dirichlet boundary conditions on $\partial\Omega_2 \setminus \Gamma_{21}$

$$u_2 = -DL_{\Gamma_{21},2}u_2 + SL_{\partial\Omega_2,2}\partial_{n_2}u_2$$

leads upon application of Dirichlet traces to the identity

$$Y^2 = S^{-1}_{\partial\Omega_2,2}\left(\frac{1}{2}I + K_{\Gamma_{21},2}\right). \tag{7.5}$$

The invertibility of the operators $S_{\partial\Omega_2,2}$ in the equation above, and hence the well posedness of the DtN operator Y^2, can be guaranteed provided the subdomain Ω_2 is small enough (typically less than one wavelength across). A simple solution that would allow one to consider subdomains of any size is to consider DtN operators $Y^{2,c}$ corresponding to complex wavenumbers $k_2 + i\sigma_2,\ \sigma_2 > 0$ instead of the operators Y^2. Using these operators, we can define a transmission operator on the interface $\partial\Omega_2$ in the form

$$\mathcal{T}_1^{DtN} = Y^{2,c}|_{\Gamma_{21}} + Y^0|_{\Gamma_{01}} \tag{7.6}$$

and similar transmission operators on the interfaces $\partial\Omega_1$ and $\partial\Omega_0$ respectively. We then match DtN Robin boundary conditions (DtNR) on the subdomain interfaces

$$\partial_{n_1}u_1 + \mathcal{T}_1^{DtN}u_1 = (\partial_{n_j}u_j + \delta_j^0\partial_{n_j}u^{inc}) + \mathcal{T}_1^{DtN}(u_j + \delta_j^0 u^{inc}),\ j \in \{0,2\}. \tag{7.7}$$

Similar generalized impedance operators can be defined for the domains Ω_0 and Ω_2 and then incorporated in a DDM algorithm that computes the generalized Robin data

$$f_j^g := (\partial_{n_j}u_j + \mathcal{T}_j^{DtN}u_j)|_{\partial\Omega_j},\ 0 \le j$$

by making use of suitably defined generalized RtR maps $\mathcal{S}^{g,j}$. We also will consider DDM that rely on approximations of the DtN operators given by the hypersingular operators. These give rise to transmission operators

$$\mathcal{T}_1 = Z_0|_{\Gamma_{10}} + Z_2|_{\Gamma_{12}} = -2N_{k_0+i\sigma_0}|_{\Gamma_{10}} - 2N_{k_2+i\sigma_2}|_{\Gamma_{12}}.$$

However, the restriction of boundary integral operators to an open arc is problematic, and a clean way to define transmission operators is given by

$$\mathcal{T}_1 = -2\chi_{10}N_{k_0+i\sigma_0}\chi_{10} - 2\chi_{12}N_{k_2+i\sigma_2}\chi_{12} \tag{7.8}$$

where χ_{10} is a smooth cutoff function supported on Γ_{10} and χ_{12} is a smooth cutoff function supported on Γ_{12}. We refer to the ensuing DDM with transmission operators defined in Equation (7.8) by the acronym DDM N.

7.3 DDM for One-dimension

In this section, we consider DDM for the Helmholtz equation in one dimension. More precisely, we consider the Helmholtz equation

$$\begin{aligned} u''(x) + (k(x))^2 u(x) &= 0 \quad \text{in} \quad (a,b) \\ u(a) = A \qquad &\text{and} \quad u(b) = B \end{aligned} \tag{7.9}$$

where the wavenumber $k(x)$ is a piecewise constant function, that is

$$k(x) = k_j \quad x \in (a_j, a_{j+1}), \quad \cup_{j=0}^{N+1}[a_j, a_{j+1}] = [a,b]$$

and u and u' are continuous at $a_j, j = 0, \ldots, N+1$. We note that we do not require that the wavenumbers k_j be necessarily different on adjacent intervals. The classical DDM formulation of the Helmholtz equation above can be written in the form

$$\begin{aligned} u_j'' + k_j^2 u_j &= 0 \quad \text{in} \quad (a_j, a_{j+1}) \\ f_{j,j-1} := (-u_j' + i\eta\, u_j)|_{x=a_j} &= (-u_{j-1}' + i\eta\, u_{j-1})|_{x=a_j} \\ f_{j,j+1} := (u_j' + i\eta\, u_j)|_{x=a_{j+1}} &= (u_{j+1}' + i\eta\, u_{j+1})|_{x=a_{j+1}} \end{aligned}$$

for all $1 \leq j \leq N$ together with the end-interval equations

$$\begin{aligned} u_0'' + k_0^2 u_0 &= 0 \quad \text{in} \quad (a_0, a_1) \\ u_0(a_0) &= A \\ f_{0,1} := (u_0' + i\eta\ u_0)|_{x=a_1} &= (u_1' + i\eta\ u_1)|_{x=a_1} \end{aligned}$$

and

$$\begin{aligned} u_{N+1}'' + k_{N+1}^2 u_{N+1} &= 0 \quad \text{in} \quad (a_{N+1}, a_{N+2}) \\ f_{N+1,N} := (-u_{N+1}' + i\eta\ u_{N+1})|_{x=a_{N+1}} &= (-u_N' + i\eta\ u_N)|_{x=a_{N+1}} \\ u_{N+1}(a_{N+2}) &= B. \end{aligned}$$

To each of these Robin problems, we associate RtR maps. First, we define for $1 \leq j \leq N$ the following matrices

$$\mathcal{S}^j \begin{bmatrix} f_{j,j-1} \\ f_{j,j+1} \end{bmatrix} := \begin{bmatrix} (u_j' + i\eta\ u_j)|_{x=a_j} \\ (-u_j' + i\eta\ u_j)|_{x=a_{j+1}} \end{bmatrix}$$

then the following complex scalars

$$\mathcal{S}^0 f_{0,1} = (-u_0' + i\eta\ u_0)|_{x=a_1} + \gamma_0 A$$

and

$$\mathcal{S}^{N+1} f_{N+1,N} = (u_{N+1}' + i\eta\ u_{N+1})|_{x=a_{N+1}} + \gamma_{N+1} B.$$

Denoting $h_j = a_{j+1} - a_j$, it is a straightforward matter to compute

$$\mathcal{S}_{11}^j = \mathcal{S}_{22}^j = \frac{(k_j + \eta)^2 (e^{ik_j h_j} - e^{-ik_j h_j})}{(k_j - \eta)^2 e^{-ik_j h_j} - (k_j + \eta)^2 e^{ik_j h_j}}$$

and

$$\mathcal{S}_{12}^j = \mathcal{S}_{21}^j = -\frac{4k_j \eta}{(k_j - \eta)^2 e^{-ik_j h_j} - (k_j + \eta)^2 e^{ik_j h_j}}$$

for $1 \leq j \leq N$. We also get

$$\mathcal{S}^0 = \frac{(\eta + k_0) e^{-ik_0 h_0} - (k_0 - \eta) e^{ik_0 h_0}}{(\eta - k_0) e^{-ik_0 h_0} - (k_0 + \eta) e^{ik_0 h_0}}$$

and

$$\mathcal{S}^{N+1} = \frac{(\eta + k_{N+1})e^{-ik_{N+1}h_{N+1}} + (k_{N+1} - \eta)e^{ik_{N+1}h_{N+1}}}{(\eta - k_{N+1})e^{-ik_{N+1}h_{N+1}} - (k_{N+1} + \eta)e^{ik_{N+1}h_{N+1}}}.$$

Ordering the data $f = [f_{01}\ f_{10}\ f_{12}\ \dots f_{N+1,N}]^\top$, then the classical DDM can be written in the form $(I + A)f = g$ where the matrix $I + A$ is given in explicit form

$$I + A = \begin{bmatrix} I & -\mathcal{S}_{11}^1 & -\mathcal{S}_{12}^1 & 0 & 0 & 0 & 0 & 0 & \dots & 0 \\ -\mathcal{S}^0 & I & 0 & 0 & 0 & 0 & 0 & 0 & \dots & 0 \\ 0 & 0 & I & -\mathcal{S}_{11}^2 & -\mathcal{S}_{12}^2 & 0 & 0 & 0 & \dots & 0 \\ 0 & -\mathcal{S}_{21}^1 & -\mathcal{S}_{22}^1 & I & 0 & 0 & 0 & 0 & \dots & 0 \\ 0 & 0 & 0 & 0 & I & -\mathcal{S}_{11}^3 & -\mathcal{S}_{12}^3 & 0 & \dots & 0 \\ \dots & \dots & \dots & \dots & \dots & \dots & \dots & \dots & \dots & \dots \\ 0 & 0 & 0 & 0 & 0 & 0 & 0 & \dots & I & -\mathcal{S}^{N+1} \\ 0 & 0 & 0 & 0 & 0 & 0 & \dots & -\mathcal{S}_{21}^N & -\mathcal{S}_{22}^N & I \end{bmatrix}. \tag{7.10}$$

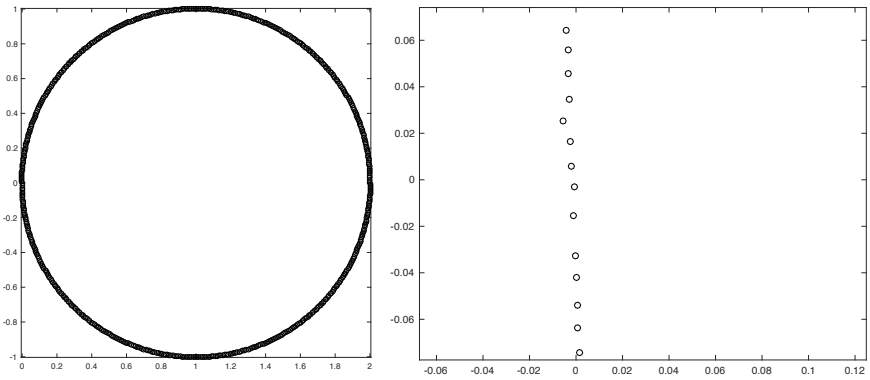

Figure 7.1 Distribution of eigenvalues of the matrix $I+A$ defined in Equation (7.10).

In Figure 7.1, we present the spectral properties of the matrix $I + A$ defined in Equation (7.10) for a case of piecewise constant wavenumber that takes four values in the interval $(0, 1)$, and a total of 300 subintervals. Here $\eta = 1$ when we solve the Helmholtz equation on the interval $[0, 1]$ with $k_0 = 1$ in $(0, 1/4)$, $k_1 = 2$ in $(1/4/, 1/2)$, $k_2 = 4$ in $(1/2, 3/4)$, and $k_3 = 8$ in $(3/4, 1)$. We further subdivided the interval $(0, 1/4)$ into 20 subintervals of equal length, the interval $(1/4/, 1/2)$ into 40 subintervals of

equal length, the interval $(1/2, 3/4)$ into 80 subintervals of equal length, and finally the interval $(3/4, 1)$ into 160 subintervals of equal length. The smallest eigenvalues of the ensuing matrix $I + A$ is of the order 10^{-3}. The spectral properties of the ensuing DDM are associated with poor behavior of GMRES iterative solvers: the eigenvalues are distributed almost uniformly on a circle of radius close to one centered at $(1, 0)$.

In the case of DtN DDM algorithm, we make use of the following DtN maps, assumed to be properly defined:

$$-v_j'(a_j) = dtn^-(a_j)v_j(a_j)$$

where v_j is the solution of the following problem

$$\begin{aligned} v_j'' + k_j^2 v_j &= 0 \quad \text{in} \quad (a_j, a_{j+1}) \\ v_j(a_j) = A_j, &\qquad v_j(a_{j+1}) = 0 \end{aligned} \tag{7.11}$$

and

$$w_j'(a_{j+1}) = dtn^+(a_{j+1})w_j(a_{j+1})$$

where w_j is the solution of the following problem

$$\begin{aligned} w_j'' + k_j^2 w_j &= 0 \quad \text{in} \quad (a_j, a_{j+1}) \\ w_j(a_j) = 0, &\qquad w_j(a_{j+1}) = A_{j+1}. \end{aligned}$$

It can be easily shown that

$$dtn^-(a_j) = dtn^+(a_{j+1}) = -ik_j \frac{e^{ik_j h_j} + e^{-k_j h_j}}{e^{-ik_j h_j} - e^{ik_j h_j}}.$$

The DtN DDM formulation of the Helmholtz equation above can be written in the form

$$\begin{aligned} u_j'' + k_j^2 u_j &= 0 \quad \text{in} \quad (a_j, a_{j+1}) \\ f_{j,j-1}^{dtn} := (-u_j' + dtn^+(a_j)u_j)|_{x=a_j} &= (-u_{j-1}' + dtn^+(a_j)\ u_{j-1})|_{x=a_j} \\ f_{j,j+1}^{dtn} := (u_j' + dtn^-(a_{j+1})\ u_j)|_{x=a_{j+1}} &= (u_{j+1}' + dtn^-(a_{j+1})\ u_{j+1})|_{x=a_{j+1}} \end{aligned}$$

for all $1 \leq j \leq N$ together with corresponding end-interval equations. Corresponding RtR DtN maps/matrices can be defined and their entries are given by

$$\mathcal{S}_{11}^{dtn,j} = \mathcal{S}_{22}^{dtn,j} = 0,$$

and

$$\begin{aligned}
\mathcal{S}_{12}^{dtn,j} &= -2ik_j \frac{dtn^-(a_j) + dtn^+(a_j)}{(dtn^-(a_j) - ik_j)(dtn^+(a_{j+1}) - ik_j)e^{-ik_j h_j} - (dtn^-(a_j) + ik_j)(dtn^+(a_{j+1}) + ik_j)e^{ik_j h_j}} \\
\mathcal{S}_{21}^{dtn,j} &= -2ik_j \frac{dtn^+(a_{j+1}) + dtn^-(a_{j+1})}{(dtn^-(a_j) - ik_j)(dtn^+(a_{j+1}) - ik_j)e^{-ik_j h_j} - (dtn^-(a_j) + ik_j)(dtn^+(a_{j+1}) + ik_j)e^{ik_j h_j}}.
\end{aligned}$$

The fact that the entries $\mathcal{S}_{11}^{dtn,j}$ and $\mathcal{S}_{22}^{dtn,j}$ are zero should not be surprising, as the use of (exact) DtN gives rise to DDM transparent boundary condition (i.e., the information propagates one-way from the subdomains). At this stage we find more intuitive to refer to $\mathcal{S}_{12}^{dtn,j}$ as to $\mathcal{S}_b^{dtn,j}$ (the subscript stands for backward, consistent with the direction in which the information propagates) and to $\mathcal{S}_{21}^{dtn,j}$ as to $\mathcal{S}_f^{dtn,j}$ (the subscript stands for forward).The DtN DDM can be written in the form $(I + A^{dtn})f^{dtn} = g^{dtn}$ where the matrix $I + A^{dtn}$ is given in explicit form

$$I + A^{dtn} = \begin{bmatrix}
I & 0 & -\mathcal{S}_b^{dtn,1} & 0 & 0 & 0 & 0 & 0 & \dots & 0 \\
0 & I & 0 & 0 & 0 & 0 & 0 & 0 & \dots & 0 \\
0 & 0 & I & 0 & -\mathcal{S}_b^{dtn,2} & 0 & 0 & 0 & \dots & 0 \\
0 & -\mathcal{S}_f^{dtn,1} & 0 & I & 0 & 0 & 0 & 0 & \dots & 0 \\
0 & 0 & 0 & 0 & I & 0 & -\mathcal{S}_b^{dtn,3} & 0 & \dots & 0 \\
\dots & \dots & \dots & \dots & \dots & \dots & \dots & \dots & \dots & \dots \\
0 & 0 & 0 & 0 & 0 & 0 & 0 & \dots & I & 0 \\
0 & 0 & 0 & 0 & 0 & 0 & \dots & -\mathcal{S}_f^{dtn,N} & 0 & I
\end{bmatrix}. \tag{7.12}$$

The matrices $I + A^{dtn}$ corresponding to the same experiment described in Figure 7.1 have only one eigenvalue $\lambda = 1$ with algebraic multiplicity $2(N+1)$ (this is the number of unknown in the DDM) and geometric multiplicity 2, that is it has only two linearly

independent eigenvectors, which turn out to be the first and the last canonical vectors in $\mathbb{R}^{2(N+1)}$. This situation was already pointed out in [27] in the case of constant wavenumber. Thus, the matrix $I + A^{dtn}$ has optimal clustering of eigenvalues. The fact that the matrix $I + A^{dtn}$ is defective accounts for the fact that the numbers of GMRES iterations required in the DtN DDM, albeit significantly smaller than those corresponding to the classical DDM, are still not consistently small throughout the frequency and contrast landscape. Interestingly, the inverse of the matrix $I+A^{dtn}$ can be computed explicitly quite easily, and the expression of it does not involve algebraic inverses. Indeed, the inverse can be written in the form [27]

$$(I + A^{dtn})^{-1} = \begin{bmatrix} I & 0 & \mathcal{S}_b^{dtn,1} & 0 & \dots & \mathcal{F}_{1,2N+2}^{-1} & 0 \\ 0 & I & 0 & 0 & \dots & 0 & 0 \\ 0 & 0 & I & 0 & \dots & \mathcal{F}_{3,2N+2}^{-1} & 0 \\ 0 & \mathcal{S}_f^{dtn,1} & 0 & I & \dots & 0 & 0 \\ \dots & \dots & \dots & \dots & \dots & \dots & \dots \\ 0 & \mathcal{F}_{2N+2,2}^{-1} & 0 & \mathcal{F}_{2N+2,4}^{-1} & \dots & 0 & I \end{bmatrix}. \tag{7.13}$$

where

$$\mathcal{F}_{mn}^{-1} = \begin{cases} -(-1)^{(n-m)/2}\Pi_{k=(m+1)/2}^{(n-1)/2}(-\mathcal{S}_b^{dtn,k}) & \text{if } m = 1, 3, \dots \quad \text{and } m < n,\ n - m = even \\ -(-1)^{(m-n)/2}\Pi_{k=m/2-1}^{n/2}(-\mathcal{S}_f^{dtn,k}) & \text{if } m = 2, 4, \dots \quad \text{and } m > n,\ m - n = even \\ 0, \quad \text{otherwise.} \end{cases} \tag{7.14}$$

The explicit form of the matrix $(I+A^{dtn})^{-1}$ described above is the basis of the double sweeping preconditioner developed by Lexing Ying and Bjorn Engquist [10]. The terminology double sweep can be explain from the formulas (7.14): the multiplication of the forward maps is illustrated in Figure 7.2, and can be interpreted as a forward subdomain sweep; the multiplication of the backward maps can be interpreted as a backward subdomain sweep, hence the double sweep terminology. The same explicit form given in Equation (7.14) is valid in higher dimensions in the case when the one

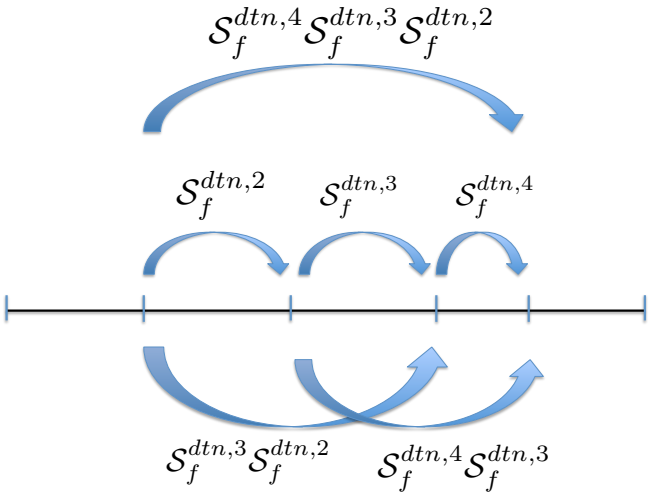

Figure 7.2 Illustration of the forward sweep.

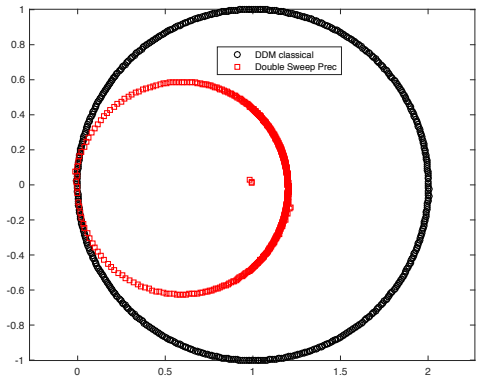

Figure 7.3 Distribution of eigenvalues of the matrix $(I + A^{dtn})^{-1}(I + A)$.

dimensional intervals are replaced by slab-like subdomains. We present in Figure 7.3 an illustration of the effect of this preconditioner on the DDM with classical Robin transmission conditions.

CHAPTER 8

NUMERICAL METHOD

We present in this chapter Nyström discretizations for the calculation of the RtR maps. First, we use sigmoidal-graded meshes to accumulate points polynomially at corners. Next, we introduce weighted versions of Neumann traces and we show how to split the kernels of weighted parametrized operators into smooth and singular components. At last, we use trigonometric interpolation to get a fully discrete approximations of boundary integral operators.

8.1 Weighted Boundary Integral Operators

We assume that the closed boundary curve Γ has corners at $\mathbf{x}_1, \mathbf{x}_2, \ldots, \mathbf{x}_P$ and that $\Gamma \backslash \{\mathbf{x}_1, \mathbf{x}_2, \ldots, \mathbf{x}_P\}$ is piecewise analytic. We assume that the boundary curve has a 2π periodic parametrization so that each of the curved segments $[\mathbf{x}_j, \mathbf{x}_{j+1}]$ is paramterized by $\mathbf{x}(t) = (x_1(w(t)), x_2(w(t)))$ with $t \in [T_j, T_{j+1}]$ (so that $\mathbf{x}_j = \mathbf{x}(T_j)$) where $0 = T_1 < T_2 < \ldots < T_P < T_{P+1} = 2\pi$ and $w : [T_j, T_{j+1}] \to [T_j, T_{j+1}],\ 1 \leq j \leq P$ is the sigmoid transform introduced by Kress

$$\begin{aligned} w(s) &= \frac{T_{j+1}[v(s)]^p + T_j[1-v(s)]^p}{[v(s)]^p + [1-v(s)]^p},\ T_j \leq s \leq T_{j+1},\ 1 \leq j \leq P \qquad (8.1) \\ v(s) &= \left(\frac{1}{p} - \frac{1}{2}\right)\left(\frac{T_j + T_{j+1} - 2s}{T_{j+1} - T_j}\right)^3 + \frac{1}{p}\,\frac{2s - T_j - T_{j+1}}{T_{j+1} - T_j} + \frac{1}{2} \end{aligned}$$

where $p \geq 2$. The function w is a smooth, increasing, bijection on each of the intervals $[T_j, T_{j+1}]$ for $1 \leq j \leq P$, with $w^{(k)}(T_j) = w^{(k)}(T_{j+1}) = 0$ for $1 \leq k \leq p-1$ and all $1 \leq j \leq P$. We also assume that $x_j : \mathbb{R} \to \mathbb{R}$ are 2π periodic with $(x_1'(t))^2 + (x_2'(t))^2 > 0$ for all t.

A central issue encountered in collocation methods of boundary integral operators in domains with corners is the possibly unbounded nature in the vicinity of

corners of the densities these operators act upon. In the case when the densities are natural Dirichlet and Neumann boundary traces of solutions of Helmholtz equation in domains with corners, which is the case with all of the formulations considered in this text, the situation is particularly pertinent to operators acting on Neumann traces. We bypass this issue by simply replacing the Neumann traces by parametrized *weighted* Neumann traces

$$\partial_n^w u(t) := \partial_n u(\mathbf{x}(t)) \; |\mathbf{x}'(t)| \tag{8.2}$$

in all of the equations that feature such quantities. In particular, the Robin data in DDM are defined *via* weighted Neumann traces. This simple procedure appears to resolve issues related to cross points (i.e., points where multiple subdomains meet) in DDM, at least according to our numerical experiments.

We introduce the graded-parameterized version of the four boundary integral operators of the Helmholtz equation. We assume that the functions φ and ψ are 2π periodic, Hölder continuous functions such that φ vanishes algebraically at T_j. The functions φ should be thought of as surrogates for parametrized weighted Neumann traces, while the functions ψ for parametrized Dirichlet traces. We start by defining the parametrized weighted single layer operator in the form

$$(S_k^w \varphi)(t) := \int_0^{2\pi} G_k(\mathbf{x}(t) - \mathbf{x}(\tau))\varphi(\tau) d\tau. \tag{8.3}$$

We define next the parametrized double layer operator in the form

$$(K_k \psi)(t) := \int_0^{2\pi} \frac{\partial G_k(\mathbf{x}(t) - \mathbf{x}(\tau))}{\partial \mathbf{n}(\mathbf{x}(\tau))} |\mathbf{x}'(\tau)| \psi(\tau) d\tau. \tag{8.4}$$

and the parametrized weighted adjoint of the double layer operator as

$$(K_k^{\top,w} \varphi)(t) := \int_0^{2\pi} |\mathbf{x}'(t)| \frac{\partial G_k(\mathbf{x}(t) - \mathbf{x}(\tau))}{\partial \mathbf{n}(\mathbf{x}(t))} \varphi(\tau) d\tau. \tag{8.5}$$

Finally, we defined the parametrized weighted hypersingular operator as

$$(N_k^w \psi)(t) := \mathrm{FP} \int_0^{2\pi} |\mathbf{x}'(t)| \; |\mathbf{x}'(\tau)| \frac{\partial^2 G_k(\mathbf{x}(t) - \mathbf{x}(\tau))}{\partial \mathbf{n}(\mathbf{x}(t)) \partial \mathbf{n}(\mathbf{x}(\tau))} \varphi(\tau) d\tau. \tag{8.6}$$

All of the kernels of the periodic integral operators defined above exhibit singularities at $\tau = t$, and the nature of these singularities is different from case to case. We present next a classical procedure that extracts the singularity of these kernels and makes possible high-order collocation discretizations of the four periodic integral operators above.

8.2 Kernel Splitting

We present a Nyström discretization of the weighted periodic integral operators that relies on (a) splitting of the kernels of the weighted parametrized operators into smooth and singular components, (b) trigonometric interpolation of the unknowns of these integral equations, and (c) analytical expressions for the integrals of products of periodic singular and weakly singular kernels and Fourier harmonics. We present first a strategy to split the kernels of the weighted parametrized integral operators featured in equations into smooth and singular components. The latter can be expressed themselves as products of *known* singular kernels and smooth kernels. We begin by looking at the operator

$$(S_k^w \varphi)(t) := \int_0^{2\pi} M_k(t,\tau)\varphi(\tau)d\tau := \int_0^{2\pi} G_k(\mathbf{x}(t) - \mathbf{x}(\tau))\varphi(\tau)d\tau, \qquad (8.7)$$

where φ it is a sufficiently smooth $2\pi-$periodic function. From the power series expansions of Hankel function,we see the kernel

$$M_k(t,\tau) = \frac{i}{2} H_0^1(k|\mathbf{x}(t) - \mathbf{x}(\tau)|)$$

We decompose the fundamental solution $H_0^{(1)} = J_0 + iN_0$ and use power series

$$J_0(z) = \sum_{n=0}^{\infty} \frac{(-1)^n}{(n!)^2} (\frac{z}{2})^{2n}$$

for the Bessel function of order zero and

$$N_0(z) = \frac{2}{\pi}(ln\frac{z}{2} + C)J_0(z) + \frac{2}{\pi}\sum_{n=1}^{\infty}(\sum_{m=1}^{\infty}\frac{1}{m})\frac{(-1)^{n+1}}{(n!)^2}(\frac{z}{2})^{2n}$$

for the Neumann function of order zero with Euler's constant C. From these series we can see that the kernel $M_k(t,\tau)$ can be expressed in the form

$$M_k(t,\tau) = M_{k,1}(t,\tau)\ln\left(4\sin^2\frac{t-\tau}{2}\right) + M_{k,2}(t,\tau)$$

with

$$\begin{aligned} M_{k,1}(t,\tau) &:= -\frac{1}{4\pi}J_0(k|\mathbf{x}(t)-\mathbf{x}(\tau)|) \\ M_{k,2}(t,\tau) &:= M_k(t,\tau) - M_{k,1}(t,\tau)\ln\left(4\sin^2\frac{t-\tau}{2}\right) \end{aligned}$$

are regular with diagonal terms

$$M_{k,1}(t,t) = -\frac{1}{4\pi}, \qquad M_{k,2}(t,t) = \frac{i}{4} - \frac{C}{2\pi} - \frac{1}{2\pi}\ln\frac{k|\mathbf{x}'(t)|}{2}.$$

The parametrized double layer operator, see (2.5), is defined as follows

$$(K_k\psi)(t) = \int_0^{2\pi} H_k(t,\tau)\psi(\tau)d\tau := \int_0^{2\pi} \frac{\partial G_k(\mathbf{x}(t)-\mathbf{x}(\tau))}{\partial \mathbf{n}(\mathbf{x}(\tau))}|\mathbf{x}'(\tau)|\psi(\tau)d\tau. \qquad (8.8)$$

We note that the integral operator K_k should be understood in the sense of Cauchy Principal Value operators; the kernel of this operator behaves as (i) $|t-\tau|^{-1}$ when $t \to T_j, t < T_j$ and $\tau \to T_j,\ \tau > T_j$ for $2 \le j \le P$ and as (ii) $(|t-\tau| \mod 2\pi)^{-1}$ when $t \to T_1 = 0$ and $\tau \to T_{P+1} = 2\pi$ (that is when $\mathbf{x}(t)$ and $\mathbf{x}(\tau)$ approach a corner from different sides). It is possible to represent K_k in terms of operators with weakly singular kernels. In order to do so, let us define $G_0(\mathbf{z}) := -\frac{1}{2\pi}\ln|\mathbf{z}|$ and express K_k in the form

$$\begin{aligned} (K_k\psi)(t) &= \int_0^{2\pi} \frac{\partial G_k(\mathbf{x}(t)-\mathbf{x}(\tau)) - G_0(\mathbf{x}(t)-\mathbf{x}(\tau))}{\partial \mathbf{n}(\mathbf{x}(\tau))}|\mathbf{x}'(\tau)|\psi(\tau)d\tau \\ &+ \int_0^{2\pi} \frac{G_0(\mathbf{x}(t)-\mathbf{x}(\tau))}{\partial \mathbf{n}(\mathbf{x}(\tau))}|\mathbf{x}'(\tau)|(\psi(\tau)-\psi(t))d\tau \\ &+ \psi(t)\int_0^{2\pi} \frac{G_0(\mathbf{x}(t)-\mathbf{x}(\tau))}{\partial \mathbf{n}(\mathbf{x}(\tau))}|\mathbf{x}'(\tau)|d\tau. \end{aligned}$$

We note that the integrands of the first two integral operators in the right hand side of the previous equation are weakly singular (they have a logarithmic singularity when

$t = \tau$); for the second integral this is because ψ is assumed to be Hölder continuous. We denote by

$$a(t) := \int_0^{2\pi} \frac{G_0(\mathbf{x}(t) - \mathbf{x}(\tau))}{\partial \mathbf{n}(\mathbf{x}(\tau))} |\mathbf{x}'(\tau)| d\tau = \begin{cases} -\frac{1}{2} & \text{if t} \in [0, 2\pi] \setminus \{\mathrm{T}_1, \ldots, \mathrm{T}_\mathrm{P}\} \\ -\frac{\gamma_j}{2\pi} & \text{if t} = \mathrm{T_j}, 1 \leq \mathrm{j} \leq \mathrm{P}. \end{cases}$$

and we get a simplified representation for the operator K_k in the form

$$(K_k \psi)(t) = \int_0^{2\pi} \frac{\partial G_k(\mathbf{x}(t) - \mathbf{x}(\tau))}{\partial \mathbf{n}(\mathbf{x}(\tau))} |\mathbf{x}'(\tau)| \psi(\tau) d\tau - \psi(t) \left(\int_0^{2\pi} \frac{\partial G_0(\mathbf{x}(t) - \mathbf{x}(\tau))}{\partial \mathbf{n}(\mathbf{x}(\tau))} |\mathbf{x}'(\tau)| d\tau \right) + a(t). \tag{8.9}$$

The kernels of the operators that enter the last expression of the operator K_k can be expressed as

$$H_k(t, \tau) := \frac{ik}{4} \nu(\tau) \cdot [\mathbf{x}(t) - \mathbf{x}(\tau)] \frac{H_1^{(1)}(k|\mathbf{x}(t) - \mathbf{x}(\tau)|)}{|\mathbf{x}(t) - \mathbf{x}(\tau)|},$$

which, in turn, can be written as

$$H_k(t, \tau) = H_{k,1}(t, \tau) \ln \left(4 \sin^2 \frac{t - \tau}{2} \right) + H_{k,2}(t, \tau)$$

with

$$\begin{aligned} H_{k,1}(t, \tau) &:= -\frac{k}{4\pi} \nu(\tau) \cdot [\mathbf{x}(t) - \mathbf{x}(\tau)] \frac{J_1(k|\mathbf{x}(t) - \mathbf{x}(\tau)|)}{|\mathbf{x}(t) - \mathbf{x}(\tau)|} \\ H_{k,2}(t, \tau) &:= H_k(t, \tau) - H_{k,1}(t, \tau) \ln \left(4 \sin^2 \frac{t - \tau}{2} \right) \end{aligned}$$

are regular with diagonal terms

$$H_{k,1}(t, t) = 0, \qquad H_{k,2}(t, t) = \frac{1}{4\pi} \frac{\nu(t) \cdot \mathbf{x}''(t)}{|\mathbf{x}'(t)|^2}.$$

It can be easily seen that the kernel of the second operator in Equation (8.9) is given by

$$H_0(t, \tau) = \frac{1}{2\pi} \frac{\nu(\tau) \cdot [\mathbf{x}(t) - \mathbf{x}(\tau)]}{|\mathbf{x}(t) - \mathbf{x}(\tau)|^2}, \qquad H_0(t, t) = -\frac{1}{4\pi} \frac{\nu(t) \cdot \mathbf{x}''(t)}{|\mathbf{x}'(t)|^2},$$

and thus $H_{k,2}(t, t) + H_0(t, t)$ is not singular even at corner points (where $|\mathbf{x}'| = 0$).

The graded-parametrized adjoint of the double layer cf. (2.6) is given by

$$(K_k^{\top,w}\varphi)(t) = \int_0^{2\pi} H_k^{\top}(t,\tau)\varphi(\tau)d\tau := \int_0^{2\pi} |\mathbf{x}'(t)| \frac{\partial G_k(\mathbf{x}(t)-\mathbf{x}(\tau))}{\partial \mathbf{n}(\mathbf{x}(t))}\varphi(\tau)d\tau. \quad (8.10)$$

Here

$$H_k^{\top}(t,\tau) := \frac{ik}{4}\nu(t)\cdot[\mathbf{x}(\tau)-\mathbf{x}(t)]\frac{H_1^{(1)}(k|\mathbf{x}(t)-\mathbf{x}(\tau)|)}{|\mathbf{x}(t)-\mathbf{x}(\tau)|},$$

where $\nu(t) = (x_2'(t), -x_1'(t))$. The kernel $K_k^{\top}(t,\tau)$ can be expressed in the form

$$H_k^{\top}(t,\tau) = H_{k,1}^{\top}(t,\tau)\ln\left(4\sin^2\frac{t-\tau}{2}\right) + H_{k,2}^{\top}(t,\tau)$$

with

$$\begin{aligned} H_{k,1}^{\top}(t,\tau) &:= -\frac{k}{4\pi}\nu(t)\cdot[\mathbf{x}(\tau)-\mathbf{x}(t)]\frac{J_1(k|\mathbf{x}(t)-\mathbf{x}(\tau)|)}{|\mathbf{x}(t)-\mathbf{x}(\tau)|} \\ H_{k,2}^{\top}(t,\tau) &:= H_k^{\top}(t,\tau) - H_{k,1}^{\top}(t,\tau)\ln\left(4\sin^2\frac{t-\tau}{2}\right) \end{aligned}$$

are regular with diagonal terms

$$H_{k,1}^{\top}(t,t) = 0, \qquad H_{k,2}^{\top}(t,t) = \frac{1}{4\pi}\frac{\nu(t)\cdot\mathbf{x}''(t)}{|\mathbf{x}'(t)|^2}.$$

A simple calculation shows that $H_{k,2}^{\top}(t,t)$ is infinite when $w'(t) = 0$. However, it is immediate to see that $H_k^{\top}(t,\tau) = H_k(\tau,t)$, so in practice we use the transpose of the matrix corresponding to the operator K_k. Finally, for the graded-parametrized version of the hypersingular operator N_k, we add and subtract $\frac{1}{4\pi}\ln(4\sin^2((t-\tau)/2)$ to get

$$(N_k^w\psi)(t) = -\mathrm{PV}\frac{1}{4\pi}\int_0^{2\pi}\cot\frac{t-\tau}{2}\,\psi'(\tau)\,\mathrm{d}\tau + \int_0^{2\pi} Q_k(t,\tau)\psi(\tau)\,\mathrm{d}\tau + \int_0^{2\pi} D_k(t,\tau)\psi'(\tau)\,\mathrm{d}\tau \quad (8.11)$$

with

$$Q_k(t,\tau) := k^2 M_k(t,\tau)(\mathbf{x}'(t))\cdot\ \mathbf{x}'(\tau)) \quad (8.12)$$

$$D_k(t,\tau) := \frac{\partial}{\partial t}\left(\frac{1}{4\pi}\ln\left(\sin^2\frac{t-\tau}{2}\right) + M_k(t,\tau)\right). \quad (8.13)$$

Note we have used

$$|\mathbf{x}'(t)||\mathbf{x}'(\tau)|(\mathbf{n}(\mathbf{x}(t))\cdot\mathbf{n}(\mathbf{x}(\tau)) = (\mathbf{x}'(t))\cdot\ \mathbf{x}'(\tau))).$$

The kernel Q_k can be treated similarly to the kernel M_k. On the other hand, a simple calculation gives that

$$D_k(t,\tau) = D_{k,1}(t,\tau)\ln\left(4\sin^2\frac{t-\tau}{2}\right) + D_{k,2}(t,\tau)$$

where

$$\begin{aligned} D_{k,1}(t,\tau) &:= -\frac{k}{4\pi}\mathbf{x}'(t)\cdot[\mathbf{x}(t)-\mathbf{x}(\tau)]\frac{J_1(k|\mathbf{x}(t)-\mathbf{x}(\tau)|)}{|\mathbf{x}(t)-\mathbf{x}(\tau)|} \\ D_{k,2}(t,\tau) &:= D_k(t,\tau) - D_{k,1}(t,\tau)\ln\left(4\sin^2\frac{t-\tau}{2}\right) \end{aligned}$$

are regular with diagonal terms

$$D_{k,1}(t,t) = 0, \qquad D_{k,2}(t,t) = -\frac{1}{4\pi}\frac{\mathbf{x}'(t)\cdot\mathbf{x}''(t)}{|\mathbf{x}'(t)|^2}.$$

Again, $D_{k,2}(t,t)$ is infinite at corners, but the trapezoidal rule can still be applied since that term is multiplied by $\psi'(t)$ which vanishes at the corners.

8.3 Trigonometric Interpolation

Once having split the kernels of the periodic integral operators according to the prescriptions above, we use trigonometric interpolation of all of the regular quantities, and explicit quadratures for the singular integrations that need be performed. To this end, we choose an equi-spaced splitting of the interval $[0, 2\pi]$ into $2n = 2PN$ points so that each subinterval $[T_j, T_{j+1}],\ 1 \le j \le P$ is split into $2N$ equi-distant points so that each of the end points T_j correspond to mesh points. We thus consider the equi-spaced collocation points $\{t_0^{(n)}, t_1^{(n)}, \ldots, t_{2n-1}^{(n)}\}$ such that $T_j = t_{j-1}^{(n)} = \frac{(j-1)\pi}{n}$ for all $1 \le j \le P$. With respect to these nodal points, the interpolation problem in the space $\mathbb{T}_n$ of trigonometric polynomials of the form

$$v(t) = \sum_{m=0}^{n} a_m \cos mt + \sum_{m=1}^{n-1} b_m \sin mt$$

is uniquely solvable [19]. We denote by $P_n : C[0, 2\pi] \to \mathbb{T}_n$ the corresponding trigonometric polynomial interpolation operator. We use the quadrature rules [18]

$$\begin{aligned}\int_0^{2\pi} \ln\left(4\sin^2\frac{t-\tau}{2}\right) f(\tau)d\tau &\approx \int_0^{2\pi} \ln\left(4\sin^2\frac{t-\tau}{2}\right)(P_n f)(\tau)d\tau \\ &= \sum_{i=0}^{2n-1} R_i^{(n)}(t) f(t_i^{(n)}) \end{aligned} \tag{8.14}$$

where the expressions $R_j^{(n)}(t)$ are given by

$$R_i^{(n)}(t) = -\frac{2\pi}{n}\sum_{m=1}^{n-1}\frac{1}{m}\cos m(t-t_i^{(n)}) - \frac{\pi}{n^2}\cos n(t-t_i^{(n)}).$$

$$R_i^{(n)}(0) = -\frac{2\pi}{n}\sum_{m=1}^{n-1}\frac{1}{m}\cos\frac{mj\pi}{n} + \frac{(-1)^j\pi}{n^2}.$$

We also use the trapezoidal rule

$$\int_0^{2\pi} f(\tau)d\tau \approx \int_0^{2\pi}(P_n f)(\tau)d\tau = \frac{\pi}{n}\sum_{i=0}^{2n-1} f(t_i^{(n)}). \tag{8.15}$$

We also use the quadrature rule [18]

$$\begin{aligned}\frac{1}{4\pi}\int_0^{2\pi}\cot\frac{\tau-t}{2}f'(\tau)d\tau &\approx \frac{1}{4\pi}\int_0^{2\pi}\cot\frac{\tau-t}{2}(P_n f)(\tau)d\tau \\ &= \sum_{i=0}^{2n-1} T_i^{(n)}(t) f(t_i^{(n)}) \end{aligned} \tag{8.16}$$

where

$$T_i^{(n)}(t) = -\frac{1}{2n}\sum_{m=1}^{n-1} m\cos m(t-t_i^{(n)}) - \frac{1}{4}\cos n(t-t_i^{(n)}).$$

The derivatives in Equation (8.11) are effected by differentiation of the global trigonometric interpolant of the densities. This can be pursued either by means of Fast Fourier Transforms (FFTs) or using the Fourier differentiation matrix $D^{(n)}$ whose entries are given by $D^{(n)}(i,j) = \frac{1}{2}(-1)^{i+j}\cot\left(\frac{(i-j)\pi}{n}\right)$, $i \neq j$ and $D^{(n)}(i,i) = 0$.

In order to avoid dealing with values at corner points of the weighted quantities $\gamma_N^w u$ and μ^w in equations, we choose equi-spaced piece-wise meshes $t_\ell^{s,(j)}$ that are shifted versions of the meshes $t_\ell^{(j)}$ by a factor $h_j/2$. All of the interpolatory quadratures presented above still apply for the shifted meshes.

In order to avoid complications related to singularities at junction/cross points, we replace in the DDM algorithm the RtR maps by *weighted* parametrized counterparts

$$\mathcal{S}^{j,w}(|\mathbf{x}'_j|\partial_{n_j}u_j - i\eta\ \alpha_j^{-1}\ u_j) := |\mathbf{x}'_j|\partial_{n_j}u_j + i\eta\ \alpha_j^{-1}\ u_j.$$

Collocated discretizations of the latter weighted RtR maps can be easily computed through a simple modification of the methodology introduced in [26] and recounted above. Nevertheless, the representation of RtR maps in terms of BIO requires use of inverses of the operators $\mathcal{A}_j$. In order for the DDM algorithm to be efficient, the electric/acoustic sizes of subdomains Ω_j should be amenable to application of direct linear algebra solvers for calculations of the inverses of the collocation of the matrices $\mathcal{A}_j$. The discretization of the weighted RtR maps corresponding to each domain $\partial\Omega_j$ is thus constructed as $N_j \times N_j$ collocation matrices $\mathcal{S}^j_{N_j}$. Specifically, each subdomain boundary $\partial\Omega_j$ is assumed to be a piecewise smooth closed curve. Graded meshes produced by means sigmoid transforms [17] that accumulate points polynomially toward corner and multiple junction points on $\partial\Omega_j$ are utilized. For each of the subdomains Ω_j, $j = 0, 1, 2$, we thus obtain graded meshes denoted by

$$L_j := \{\mathbf{x}^j_m, m = 0, \ldots, N_j - 1\} \quad \text{on} \quad \partial\Omega_j,$$

with the same polynomial degree of the sigmoid transforms on all subdomains. All meshes in the parameter space $[0, 2\pi]$ are shifted by the same amount so that none of the grid points on the skeleton corresponds to a triple/multiple junction or a corner point. Using graded meshes that avoid corner points and the classical singular quadratures of Kusmaul and Martensen [20, 21], we perform the Nyström discretization presented in [9] to produce high-order $N_j \times N_j$ collocation matrix approximations of the four BIO in (2.4). In what follows we present specific details

on how to use the Nyström discretization of the BIOs to produce discretizations of the various formulations (MTF and DDM) considered in this text.

On a common interface $\Gamma_{j\ell}$ between two subdomains Ω_j and Ω_ℓ that share an edge, the grid points corresponding to the mesh in each subdomain may coincide or not. We refer to the former case as (1) conforming meshes, and the latter case as (2) non-conforming meshes. In case (1), the discretization of the various projection/extension operators in the definition of the $X_{j\ell}$ is straightforward, as it amounts to multiplication by matrices made up of zero and identity blocks. In case (2), the discretization of the operators $X_{j\ell}$ require incorporation of interpolation/restriction operators which can be easily performed in the trigonometric polynomial setting. Indeed, the transfer of information from the $\partial\Omega_j$ mesh L_j of size N_j to the $\partial\Omega_j$ mesh $L_{j'}$ of size $N_{j'}$ with $N_j < N_{j'}$ can be performed via zero padding in the Fourier space; the reversed information exchange can be also readily effected via Fourier space restriction operators.

We present a detailed algorithmic description of the DDM considered in this paper.

1 Offline: For each subdomain Ω_j, discretize all the BIO that feature in formula (4.1) corresponding to each boundary $\partial\Omega_j$ using Nyström discretizations. The discretization of each BIO in formula (4.1) results in a collocation matrix of size $N_j \times N_j$, whose computational cost is $\mathcal{O}(N_j^2)$;

2 Offline: Compute all the collocated subdomain RtR matrices $\mathcal{S}_{N_j}^j$ using formula (4.3) with $Z_j = ik_0$ and LU factorizations. Given the matrix inversion in (4.3), the cost of evaluating each subdomain RtR map is $\mathcal{O}(N_j^3)$;

3 Solution: Set up the DDM linear system according to formula (7.3) and solve for the Robin data f^N defined on the skeleton using GMRES;

4 Post-processing: Use the Robin data f^N computed in the previous step and the RtR matrices $\mathcal{S}_N^j$ to compute Cauchy data on the boundary of each subdomain Ω_j.

Algorithm 1: Description of the DDM algorithm with classical Robin boundary conditions

1 Offline: For each subdomain Ω_j, discretize the operators $\mathcal{T}_j$ defined in formulas (7.8) ;

2 Offline: For each subdomain Ω_j, discretize all the BIO that feature in formula (4.1) corresponding to each boundary $\partial\Omega_j$ using Nyström discretizations. The discretization of each BIO in formula (4.1) results in a collocation matrix of size $N_j \times N_j$, whose computational cost is $\mathcal{O}(N_j^2)$;

3 Offline: Compute all the collocated subdomain Robin-to-Robin matrices $\mathcal{S}_N^j$ using formula (4.3) with $Z_j = \mathcal{T}_j$ and LU factorizations. Given the matrix inversion in (4.3), the cost of evaluating each subdomain RtR map is $\mathcal{O}(N_j^3)$;

4 Solution: Set up the DDM linear system according to formula (7.3) and solve for the Robin data f^N defined on the skeleton using GMRES;

5 Post-processing: Use the Robin data f^N computed in the previous step and the RtR matrices $\mathcal{S}_N^j$ to compute Cauchy data on the boundary of each subdomain Ω_j.

Algorithm 2: Description of the DDM N algorithm.

1 Offline: For each subdomain Ω_j, compute collocated approximations of the complexified DtN operators $Y^{j,c}$ *via* Equation (7.5). This step requires construction of collocation matrices for the discretization of complexified single and double layer operators, as well as inverses of the former. The computational cost of this stage is $\mathcal{O}(N_j^3)$;

2 Offline: Use the DtN matrices computed in the previous step and compute discretizations the operators $\mathcal{T}_j^{DtN}$ defined in formulas (7.6). For a given subdomain, DtN matrices of adjacent subdomains are needed. The application of the projections in formula (7.6) simply amounts to extraction if suitable blocks from the DtN matrices;

3 Offline: For each subdomain Ω_j, discretize all the BIO that feature in formula (4.1) corresponding to each boundary $\partial\Omega_j$ using Nyström discretizations. The discretization of each BIO in formula (4.1) results in a collocation matrix of size $N_j \times N_j$, whose computational cost is $\mathcal{O}(N_j^2)$;

4 Offline: Compute all the collocated subdomain Robin-to-Robin matrices $\mathcal{S}_N^j$ using formula (4.3) with $Z_j = \mathcal{T}_j^{DtN}$ and LU factorizations. Given the matrix inversion in (4.3), the cost of evaluating each subdomain RtR map is $\mathcal{O}(N_j^3)$;

5 Solution: Set up the DDM linear system according to formula (7.3) and solve for the Robin data f^N defined on the skeleton using GMRES;

6 Post-processing: Use the Robin data f^N computed in the previous step and the RtR matrices $\mathcal{S}_N^j$ to compute Cauchy data on the boundary of each subdomain Ω_j.

Algorithm 3: Description of the DDM DtNR algorithm.

CHAPTER 9

NUMERICAL RESULTS

We present in this section a variety of numerical results that demonstrate the properties of the MTF and DDM formulations considered in this text. For every scattering experiment we consider plane-wave incidence u^{inc} and we present maximum far-field errors, that is we choose sufficiently many directions and for each direction we compute the far-field amplitude defined as

$$u^0(x) = \frac{e^{ik|x|}}{\sqrt{x}} \left(u^1_\infty(\hat{x}) + O(|x|^{-1}) \right), |x| \to \infty. \tag{9.1}$$

The maximum far-filed errors were evaluated through comparisons of the numerical solutions $u^{0,calc}_\infty$ corresponding to reference solutions $u^{0,ref}_\infty$

$$\varepsilon_\infty = \max |u^{0,calc}_\infty(\hat{x}) - u^{0,ref}_\infty(\hat{x})| \tag{9.2}$$

We first present in Table 9.1 the high-order convergence of the Nyström method for the MTF formulation with two subdomains, that is a classical transmission problem. We considered a square object of side equal to 2 and plane-wave incident fields of direction $\mathbf{d} = (1, 0)$.

We start in Table 9.2 with an illustration of the accuracy of the Nyström discretizations of the CFIESK and various DDM formulations of the transmission problem (2.1). We use the case of scattering from an L-shaped domain with $\omega = 2$, $\varepsilon_0 = 1$, and $\varepsilon_1 = 4$ with $\alpha_j = 1, j = 0, 1$. We considered a GMRES residual of 10^{-12} in all the tests presented in the Table. CFIESK formulations uses twice as many unknowns as the DDM formulations. We note that the CFIESK and DDM with transmission operators Z_j and Z^{PS}_j exhibit iterative behaviors corresponding

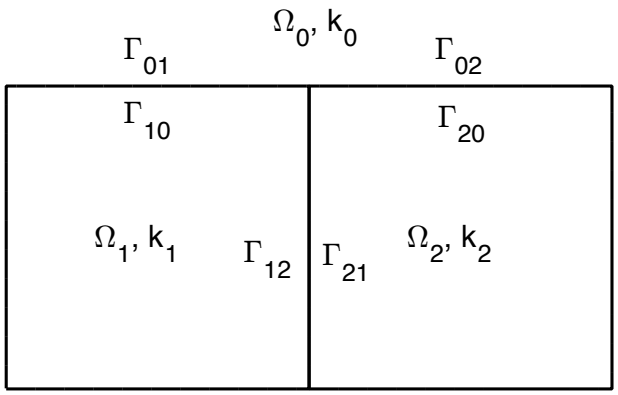

Figure 9.1 Two domain composite scatterer.

Table 9.1 High-order Convergence of the Nyström Method for MTF

Unknowns	ε_∞
64	8.9×10^{-5}
128	1.1×10^{-5}
256	1.4×10^{-6}
512	1.7×10^{-7}
1024	2.1×10^{-8}

Table 9.2 Far-field Errors Computed using Various Formulations in the Case of Scattering from An L-shaped Domain

Unknowns	CFIESK		DDM $Z_j, j = 0, 1$		DDM $Z_j^{PS}, j = 0, 1$		DDM $Z_j^a, j = 0, 1$	
	It	ε_∞	It	ε_∞	It	ε_∞	It	ε_∞
72	51	9.2×10^{-4}	26	4.3×10^{-3}	30	4.3×10^{-3}	54	4.3×10^{-3}
144	51	5.6×10^{-6}	26	3.4×10^{-4}	30	3.4×10^{-4}	66	3.4×10^{-4}
288	51	3.9×10^{-7}	26	3.9×10^{-5}	30	3.9×10^{-5}	74	3.9×10^{-5}
572	51	2.5×10^{-8}	25	4.1×10^{-6}	30	4.1×10^{-6}	87	4.1×10^{-6}
1144	51	1.6×10^{-9}	25	2.6×10^{-7}	30	2.6×10^{-7}	104	2.6×10^{-7}

to second kind formulations, while the DDM with transmission operators Z_j^a behave like first kind formulations. Also, the solvers based on CFIESK formulations are more accurate than the DDM solvers, and the accuracy of the latter formulations is virtually independent of the choice of transmission operators.

In Tables 9.3 and 9.4, we present the behavior of the various formulations for the transmission problem (2.1) as a function of frequency in the case of high-contrast material properties, that is $\varepsilon_0 = 1$ and $\varepsilon_1 = 16$ and two scatterers: a square of size 4 in Table 9.3 and an L-shaped domain of size 4 in Table 9.4. The DDM discretization used conforming meshes $64, 128, 256, 512, 1024$, and respectively 2048 unknowns; CFIESK formulations used twice as many unknowns. In Table 9.3, the numbers of iterations required by the DDM solvers with transmission operators $Z_j, j = 0, 1$ were 13, 15, 14, 19, 23, and respectively 31 in the case when $\alpha_j = \varepsilon_j^{-1}, j = 0, 1$. In Table 9.4, the numbers of iterations required by the DDM solvers with transmission operators $Z_j, j = 0, 1$ were 21, 23, 21, 23, 29, and respectively 37 in the case when $\alpha_j = \varepsilon_j^{-1}, j = 0, 1$. In order to solve smaller-sized systems, we can eliminate the generalized Robin data f_1 from the DDM system and derive the equation

$$(I - \mathcal{S}^1\mathcal{S}^0)f_0 = (-\alpha\partial_{n_0}u^{inc} + Z_1u^{inc}) + \mathcal{S}^1(\alpha\partial_{n_0}u^{inc} + Z_0u^{inc}) \quad \text{on } \Gamma. \tag{9.3}$$

Table 9.3 Far-field Errors Computed using Various Formulations in the Case of Scattering From a Square of Size 4 with $\varepsilon_0 = 1$ and $\varepsilon_1 = 16$ with $\alpha_j = 1, j = 0, 1$

ω	CFIESK		DDM $Z_j, j = 0, 1$		DDM $Z_j^{PS}, j = 0, 1$		DDM $Z_j^a, j = 0, 1$	
	It	ε_∞	It	ε_∞	It	ε_∞	It	ε_∞
1	24	3.1×10^{-4}	10	5.2×10^{-3}	10	5.1×10^{-3}	20	5.0×10^{-3}
2	39	8.2×10^{-4}	11	1.0×10^{-3}	12	9.9×10^{-4}	28	1.1×10^{-3}
4	93	2.3×10^{-3}	12	1.2×10^{-3}	17	1.4×10^{-3}	46	1.3×10^{-3}
8	162	6.3×10^{-3}	10	2.1×10^{-3}	19	2.2×10^{-3}	84	2.1×10^{-3}
16	333	7.6×10^{-3}	11	4.5×10^{-3}	29	4.2×10^{-3}	151	4.1×10^{-3}
32	565	1.2×10^{-2}	13	2.9×10^{-3}	56	2.8×10^{-3}	253	2.9×10^{-3}

Table 9.4 Far-field Errors Computed using Various Formulations in the Case of Scattering from a L-shaped Domain of Size 4 with $\varepsilon_0 = 1$ and $\varepsilon_1 = 16$ with $\alpha_j = 1, j = 0, 1$

ω	CFIESK		DDM $Z_j, j = 0, 1$		DDM $Z_j^{PS}, j = 0, 1$		DDM $Z_j^a, j = 0, 1$	
	It	ε_∞	It	ε_∞	It	ε_∞	It	ε_∞
1	43	1.0×10^{-3}	15	4.7×10^{-3}	16	4.6×10^{-3}	31	4.6×10^{-3}
2	72	1.1×10^{-3}	15	9.0×10^{-4}	17	1.2×10^{-3}	46	8.3×10^{-4}
4	135	2.1×10^{-3}	16	2.4×10^{-3}	24	2.4×10^{-3}	81	2.3×10^{-3}
8	208	2.4×10^{-3}	15	4.0×10^{-3}	29	4.0×10^{-3}	112	4.1×10^{-3}
16	493	8.8×10^{-3}	21	8.1×10^{-3}	56	8.1×10^{-3}	276	8.0×10^{-3}
32	887	1.2×10^{-2}	22	9.6×10^{-3}	87	9.6×10^{-3}	488	9.6×10^{-3}

Once the generalized Robin data f_0 is computed from Equation (9.3), the exterior Dirichlet and Neumann traces are retrieved using the RtR operators $\mathcal{S}^0$. The interior Cauchy data is then retrieved from the boundary conditions.

Clearly, from the Table 9.5, in the case of high-frequency, high-contrast transmission problems, DDM that use conforming meshes are not the most advantageous computationally. Rather, the use of non-conforming meshes that resolve the wavenumber corresponding to each subdomain are more favorable. In the latter case, the additional computational cost to transfer the Robin data from coarser to finer meshes is negligible given that it is performed via Fourier padding.

Table 9.5 Comparison Between the Conforming and Non-conforming DDM with Transmission Operators $Z_j, j = 0, 1$ for High-contrast Transmission Problems with $\varepsilon_0 = 1$ and $\varepsilon_1 = 16$ with $\alpha_j = 1, j = 0, 1$

ω	DDM (1) $Z_j, j = 0, 1$ Square			DDM (2) $Z_j, j = 0, 1$ Square			DDM (1) $Z_j, j = 0, 1$ L-shape			DDM (1) $Z_j, j = 0, 1$ L-shape		
	N	It	ε_∞	N	It	ε_∞	N	It	ε_∞	N	It	ε_∞
4	256	10	1.2×10^{-3}	192	10	1.2×10^{-3}	256	16	2.4×10^{-3}	192	14	6.0×10^{-3}
8	512	10	2.1×10^{-3}	384	14	6.1×10^{-3}	512	15	4.0×10^{-3}	384	12	3.1×10^{-3}
16	1024	11	4.5×10^{-3}	768	16	6.7×10^{-3}	1024	21	8.1×10^{-3}	768	22	1.2×10^{-2}
32	2048	13	2.9×10^{-3}	1536	25	4.9×10^{-3}	2048	22	9.6×10^{-3}	1536	27	1.3×10^{-2}

Given that the operators Z_j^{PS} are non-local operators defined as Fourier multipliers, their discretization is challenging to finite difference/finite element discretizations. Therefore, approximations of the square root operators Z_j^{PS} more amenable to other types of discretizations were proposed in the literature. To the best of our knowledge, a good such approximation is given by

$$\sqrt{1+X} \approx e^{i\theta/2} R_p(e^{-i\theta} X) = A_0 + \sum_{j=1}^{p} \frac{A_j X}{1 + B_j X}$$

where the complex numbers A_0, A_j and B_j are given by

$$A_0 = e^{i\theta/2} R_p(e^{-i\theta} - 1), \quad A_j = \frac{e^{-i\theta/2} a_j}{(1 + b_j(e^{-i\theta} - 1))^2}, \quad B_j = \frac{e^{-i\theta} b_j}{1 + b_j(e^{-i\theta} - 1)}$$

and

$$R_p(z) = 1 + \sum_{j=1}^{p} \frac{a_j z}{1 + b_j z}$$

with

$$a_j = \frac{2}{2p+1} \sin^2\left(\frac{j\pi}{2p+1}\right) \qquad b_j = \cos^2\left(\frac{j\pi}{2p+1}\right).$$

Thus, we can also use the following transmission operators

$$Z_j^{Pade,p} = -\frac{i}{2}(k_j + i\sigma_j) \left(A_0 I - \sum_{j=1}^{p} A_j \left(\frac{\Delta_\Gamma}{(k_j + i\sigma_j)^2} \right) \left(I - B_j \left(\frac{\Delta_\Gamma}{(k_j + i\sigma_j)^2} \right) \right)^{-1} \right), \tag{9.4}$$

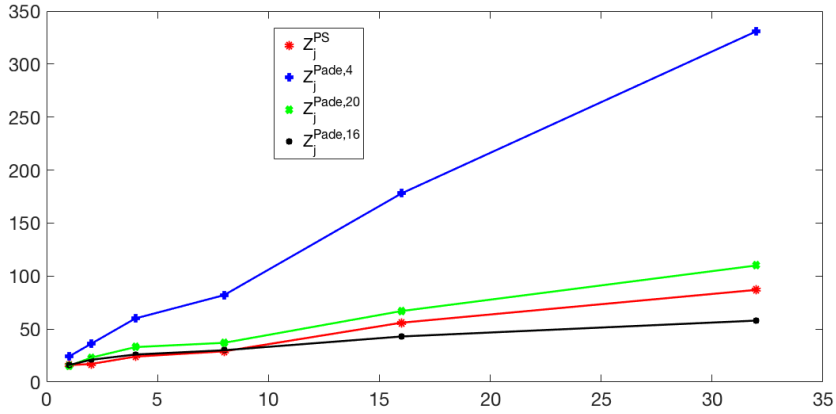

Figure 9.2 The numbers of iterations required by the DDM solvers with transmission operators $Z_j^{PS}, j = 0, 1$ as well as Padé approximations $Z_j^{Pade,p}, j = 0, 1$ for various values of p, L-shaped scatterer and the same material parameters as in Table 9.4.

where $\Delta_\Gamma = \partial_s^2$, and ∂_d is the tangential derivative on Γ. We note that the discretizations of the operators $Z_j^{Pade,p}, j = 0, 1$ defined in Equation (9.4) is relatively straightforward using trigonometric interpolants. However, their discretization requires p matrix inverses per wavenumber. We present in Figure 9.2 a comparison between the DDM iterations as a function of the Padé parameter p in the case of a L-shaped scatterer and the same material parameters as those in Table 9.4. For the configuration presented in Figure 9.2, we have found in practice that the value $p = 16$ leads to optimal iterative behavior of the DDM, but this behavior is sensitive to the values of p in the high-frequency regime. Albeit smaller values of the Padé parameter p give rise to less expensive evaluations of the transmission operators $Z_j^{Pade,p}, j = 0, 1$, they lead to large numbers of DDM iterations in the high-frequency regime.

As it can be seen from the results in Tables 9.3 and 9.4, the DDM solvers based on optimized transmission operators Z_j and Z_j^{PS} exhibit superior iterative Krylov subspace performance. Nevertheless, DDM formulations rely on discretization of RtR operators $\mathcal{S}^j$, which, in turn, rely on matrix inversions. We turn our attention next in Tables 9.6 and 9.7 to the numbers of iterations required for computation

Table 9.6 Numbers of Iterations Required for the Calculation of the RtR Operators $\mathcal{S}^j, j = 0, 1$ Corresponding to the Transmission Operators $Z_j, j = 0, 1$ in the Case of the Square Scatterer Ω_1

ω	Ω_0			Ω_1		
	$\mathcal{A}_0$ (4.2)	$\mathcal{B}_0$ (4.4)	$\mathcal{C}_0$ (4.7)	$\mathcal{A}_1$ (4.2)	$\mathcal{B}_1$ (4.4)	$\mathcal{C}_1$ (4.6)
1	13	16	37	18	21	49
2	17	21	49	26	29	70
4	24	36	84	51	56	131
8	31	49	104	83	79	217
16	35	75	143	170	142	431
32	42	125	228	263	214	793

of $\mathcal{S}^j$ corresponding to the transmission operators $Z_j, j = 0, 1$ based on the three formulations discussed in this text. Specifically, we used (1) interior/exterior formulations that require inversion of the operators $\mathcal{A}_j, j = 0, 1$ defined in Equation (4.2); (2) interior/exterior formulations that require inversion of the operators $\mathcal{B}_j, j = 0, 1$ defined in Equation (4.4); and (3) interior formulations that require inversion of the operators $\mathcal{C}_1$ defined in Equation (4.6) and exterior formulations that require inversion of the operators $\mathcal{C}_0$ defined in Equation (4.7). Although there is no theory in place for the well-posedness of boundary integral equations that involve inversion of the operators $\mathcal{B}_0$ defined in Equation (4.4), our numerical experiments suggest that it is possible to invert discretizations of those operators. As it can be seen from the results presented in Tables 9.6 and 9.7, while the numbers of iterations required to solve exterior impedance problems do not increase significantly with frequency provided that carefully defined formulations $\mathcal{A}_0$ (4.2) are used, this is no longer the case for interior impedance problems, regardless of formulation used. Similar scenarios occur for the other choices of transmission operators discussed in this text.

We present in Figure 9.3 the eigenvalue distributions of the DDM formulation with transmission operators $Z_j, j = 0, 1$ for various test-case configurations. We see

Table 9.7 Numbers of Iterations Required for the Calculation of The RtR Operators $\mathcal{S}^j, j = 0, 1$ Corresponding to The Transmission Operators $Z_j, j = 0, 1$ in the Case of The L-shaped Scatterer Ω_1

ω	Ω_0			Ω_1		
	$\mathcal{A}_0$ (4.2)	$\mathcal{B}_0$ (4.4)	$\mathcal{C}_0$ (4.7)	$\mathcal{A}_1$ (4.2)	$\mathcal{B}_1$ (4.4)	$\mathcal{C}_1$ (4.6)
1	17	22	44	24	26	67
2	22	27	58	38	42	92
4	31	39	80	66	65	160
8	34	63	131	106	94	247
16	38	104	188	218	195	473
32	45	168	309	405	333	890

the strong clustering of eigenvalues around 1, consistent with rationale for choosing transmission operators that are approximations of DtN operators. However, the operators $\mathcal{S}^0\mathcal{S}^1$ are not contraction.

In the next set of results in Table 9.8, we present the performance of the MTF and DDM solvers in the case of the composite object depicted in Figure 9.1. We take $\varepsilon_0 = 1$, $\varepsilon_1 = 64$, and $\varepsilon_2 = 256$. The numbers of unknowns required by the DDM and CFIESK formulations are 384, 768, 1536, 3072, and 6144 respectively; the MTF uses twice as many unknowns in each case. The largest size of the subdomains in these experiments is 80 wavelengths across.We report the number of GMRES iterations required by solvers based on each formulation to reach relative residuals of 10^{-4}. In the DDM algorithms the DtN maps are precomputed in an offline stage (when needed), followed by the precomputation of the RtR maps. This is a computationally intensive stage, but it can be parallelized efficiently. Per common DDM practice, the size of subdomains should be such that direct linear algebra solvers are amenable to computations of DtN and RtR maps. Thus, when the size of the subdomains is deemed too large, they can be further split into smaller subdomains. As it can be

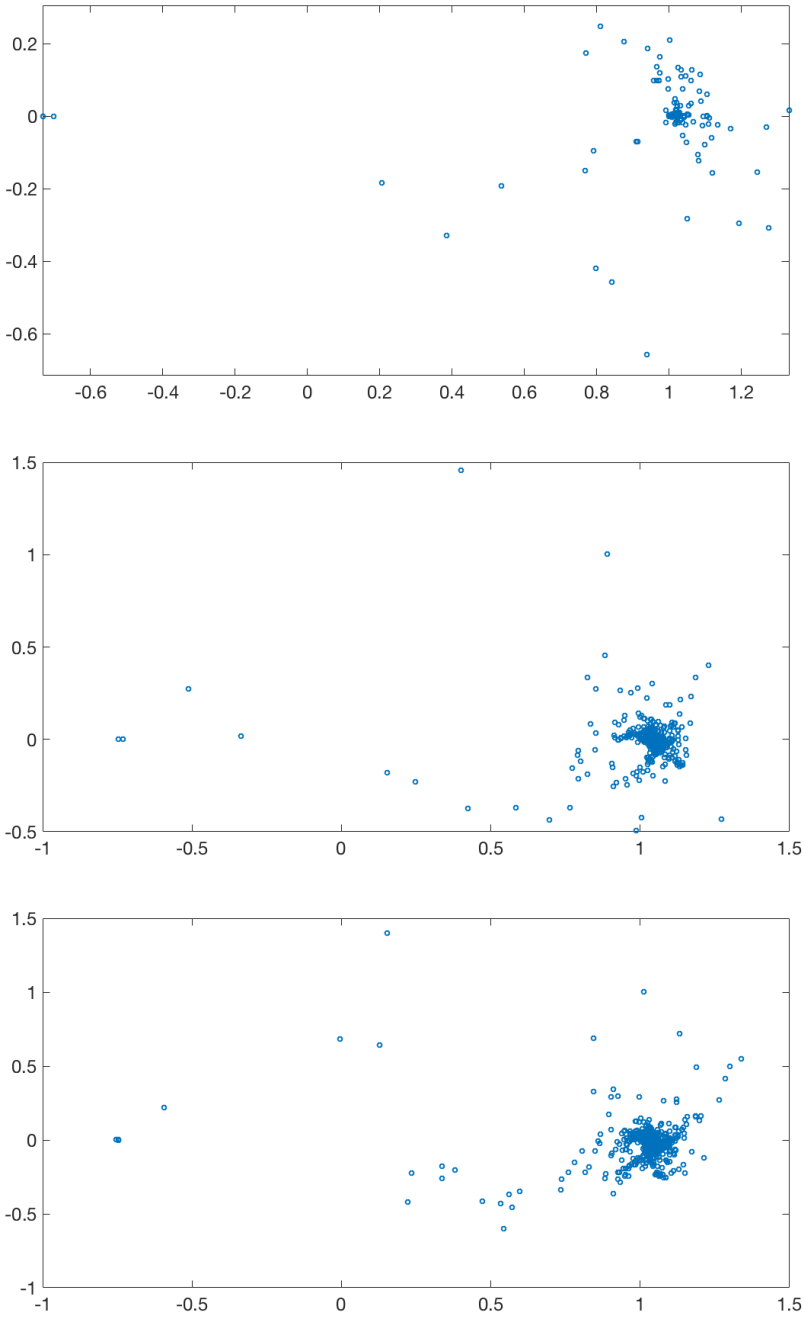

Figure 9.3 Eigenvalue distribution of the DDM formulation using Z_0 and Z_1 in case of a L-shaped domain, with $\varepsilon_0 = 1$, $\varepsilon_1 = 16$, $\alpha_j = 1, j = 0, 1$, and $\omega = 4$ (top), $\omega = 16$ (middle), and $\omega = 32$ (bottom).

Table 9.8 Performance of the Various Formulations in the Two Subdomain Case in Figure 9.1

ω	DDM		DDM N		DDM DtN		MTF		
	It	ε_∞	It	ε_∞	It	ε_∞	It MTF	It MTF Calderón	ε_∞
1	157	4.7×10^{-3}	34	6.7×10^{-3}	78	3.0×10^{-3}	169	106	6.4×10^{-3}
2	230	2.9×10^{-3}	41	5.2×10^{-3}	87	1.5×10^{-3}	303	174	3.7×10^{-3}
4	375	7.3×10^{-4}	53	1.5×10^{-3}	112	6.2×10^{-4}	560	312	1.5×10^{-3}
8	754	4.7×10^{-4}	77	1.1×10^{-3}	180	4.2×10^{-4}	1,069	586	8.5×10^{-4}
16	1,221	2.4×10^{-4}	124	1.7×10^{-3}	321	2.5×10^{-4}	1,940	1,118	9.2×10^{-4}

Table 9.9 Performance of the Various Formulations in the Four Subdomain Case in Figure 9.4

ω	DDM		DDM N		DDM DtN		MTF		
	It	ε_∞	It	ε_∞	It	ε_∞	It MTF	It MTF Calderón	ε_∞
4	266	1.6×10^{-3}	68	1.9×10^{-3}	77	2.3×10^{-3}	509	286	4.1×10^{-3}
8	470	1.1×10^{-3}	103	4.6×10^{-3}	107	4.5×10^{-3}	937	517	3.9×10^{-3}
16	907	2.3×10^{-3}	159	3.2×10^{-3}	162	3.7×10^{-3}	1,687	994	4.5×10^{-3}

seen form the results presented in Table 9.8, amongst all formulations considered the DDM N and DtN methods are best suited for iterative solvers.

We present in Table 9 the performance of different formulations considered in this text in the case of a five subdomain configuration depicted in Figure 9.4. We take $\varepsilon_0 = 1$, $\varepsilon_1 = 4$, $\varepsilon_2 = 16$, $\varepsilon_3 = 64$, and $\varepsilon_4 = 256$. The numbers of unknowns required by the DDM and CFIESK formulations are 1152, 2304 and 4608 respectively. The largest size of the subdomains in these experiments is 160 wavelengths across. Again, the DDM N formulations perform the best when used in conjunction with Krylov subspace iterative solvers. We note that the use of "exact" DtN operators instead of their cheaper approximations given by hypersingular operators does not improve the DDM iterative behavior. Given that the precomputation of DtN maps is expensive, we conclude that the DDM N are the best performing DDM formulation.

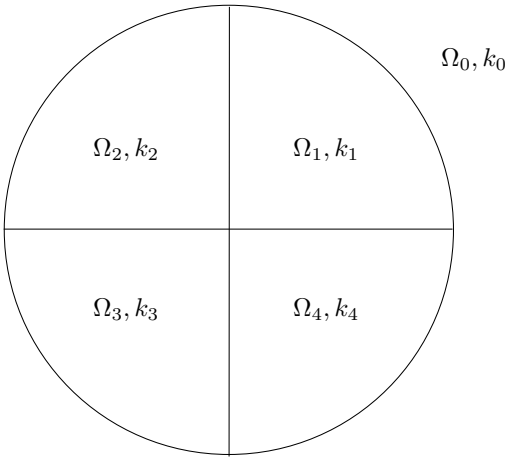

Figure 9.4 Four domain composite scatterer.

We close the numerical results section with an illustration of the eigenvalues of the DDM N formulations for the highest frequencies considered in Table 9.8 and Table 9.9 respectively. We note that the eigenvalues are more spread out than in the case of one subdomain case.

9.1 Conclusions

We presented a variety of numerical tests that showcase the superior iterative behavior of DDM with optimized transmission conditions over classical boundary integral equation formulations. For the problems considered in this dissertation, that is piece-wise constant material properties, existing boundary integral solvers can be easily be incorporated in the DDM framework. The optimal transmission operators, which are approximations of DtN operators, are also easily implementable in a BIE framework, and their computational overhead is rather negligible. The gains that can be garnered from use of DDM with optimized transmission conditions over DDM with classical Robin transmission conditions are considerable. A major advantage of DDM is the ease of parallelization. However, the performance of DDM deteriorates with the increases in the numbers of subdomains, even in the case when optimized transmission conditions are used. Since in the case of high-frequencies domain subdivisions are

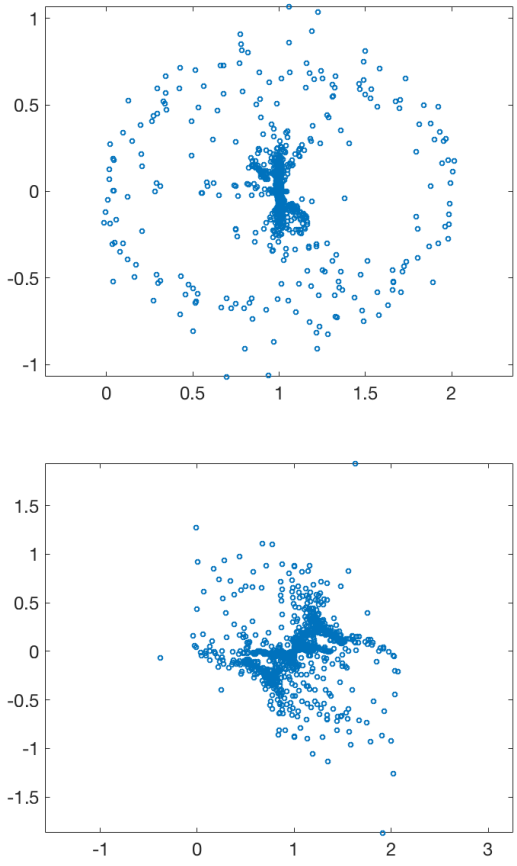

Figure 9.5 Eigenvalue distribution of the DDM N formulation using Z_0 and Z_1 in case of the two subdomain case (top) and four subdomain case (bottom) for the highest frequencies considered in Table 9.8 and Table 9.9, respectively.

necessary to maintain the efficiency of DDM, preconditioners are required. In cases when the subdomains form a layer structure, that is the adjacency graph is a tree, double sweep preconditioners were shown to be effective when the material properties of the medium do not undergo rapid transitions.

BIBLIOGRAPHY

[1] X. Antoine and M. Darbas. Alternative integral equations for the iterative solution of acoustic scattering problems. *Quart. J. Mech. Appl. Math.*, 58(1):107–128, 2005.

[2] A. Bayliss, C. I. Goldstein, and E. Turkel. An iterative method for the helmholtz equation. *J. Comput. Phys.*, 49(3):443–457, 1983.

[3] Y. Boubendir, X. Antoine, and C. Geuzaine. A quasi-optimal non-overlapping domain decomposition algorithm for the Helmholtz equation. *J. Comput. Phys.*, 231(2):262–280, 2012.

[4] Y. Boubendir, O. Bruno, C. Levadoux, and C. Turc. Integral equations requiring small numbers of Krylov-subspace iterations for two-dimensional smooth penetrable scattering problems. *Appl. Numer. Math.*, 95:82–98, 2015.

[5] X. Claeys, R. Hiptmair, and C. Jerez-Hanckes. Multitrace boundary integral equations. In *Direct and inverse problems in wave propagation and applications*, volume 14 of *Radon Ser. Comput. Appl. Math.*, pages 51–100. De Gruyter, Berlin, 2013.

[6] D. Colton and R. Kress. *Integral equation methods in scattering theory.* Pure and Applied Mathematics (New York). John Wiley & Sons Inc., New York, 1983. A Wiley-Interscience Publication.

[7] M. Costabel and E. Stephan. A direct boundary integral equation method for transmission problems. *J. Math. Anal. Appl.*, 106(2):367–413, 1985.

[8] B. Després. Décomposition de domaine et problème de Helmholtz. *C. R. Acad. Sci. Paris Sér. I Math.*, 311(6):313–316, 1990.

[9] V. Dominguez, M. Lyon, and C. Turc. Well-posed boundary integral equation formulations and nystr\" om discretizations for the solution of helmholtz transmission problems in two-dimensional lipschitz domains. *arXiv preprint arXiv:1509.04415*, 2015.

[10] B. Engquist and L. Ying. Sweeping preconditioner for the helmholtz equation: hierarchical matrix representation. *Commun. Pur. Appl. Math.*, 64(5):697–735, 2011.

[11] Y. A. Erlangga, C. Vuik, and C. W. Oosterlee. On a class of preconditioners for solving the helmholtz equation. *Appl. Numer. Math.*, 50(3):409–425, 2004.

[12] L. Escauriaza, E. B. Fabes, and G. Verchota. On a regularity theorem for weak solutions to transmission problems with internal Lipschitz boundaries. *Proc. Amer. Math. Soc.*, 115(4):1069–1076, 1992.

[13] M. J. Gander, F. Magoulès, and F. Nataf. Optimized Schwarz methods without overlap for the Helmholtz equation. *SIAM J. Sci. Comput.*, 24(1):38–60 (electronic), 2002.

[14] S. Ghanemi, F. Collino, and P. Joly. Domain decomposition method for harmonic wave equations. In *Mathematical and numerical aspects of wave propagation (Mandelieu-La Napoule, 1995)*, pages 663–672. SIAM, Philadelphia, PA, 1995.

[15] R. Hiptmair and C. Jerez-Hanckes. Multiple traces boundary integral formulation for Helmholtz transmission problems. *Adv. Comput. Math.*, 37(1):39–91, 2012.

[16] R. Hiptmair, C. Jerez-Hanckes, J.-F. Lee, and Z. Peng. Domain decomposition for boundary integral equations via local multi-trace formulations. In J. Erhel, M.J. Gander, L. Halpern, G. Pichot, T. Sassi, and O. Widlund, editors, *Domain Decomposition Methods in Science and Engineering XXI.*, volume 98 of *Lecture Notes in Computational Science and Engineering*, pages 43–58, Berlin, 2014. Springer.

[17] R. Kress. A Nyström method for boundary integral equations in domains with corners. *Numer. Math.*, 58(2):145–161, 1990.

[18] R. Kress. On the numerical solution of a hypersingular integral equation in scattering theory. *J. Comput. Appl. Math.*, 61(3):345–360, 1995.

[19] R. Kress. *Linear integral equations*, volume 82 of *Applied Mathematical Sciences*. Springer-Verlag, New York, second edition, 1999.

[20] R. Kussmaul. Ein numerisches Verfahren zur Lösung des Neumannschen Aussenraumproblems für die Helmholtzsche Schwingungsgleichung. *Computing (Arch. Elektron. Rechnen)*, 4:246–273, 1969.

[21] E. Martensen. Über eine Methode zum räumlichen Neumannschen Problem mit einer Anwendung für torusartige Berandungen. *Acta Math.*, 109:75–135, 1963.

[22] F. Nataf. Interface connections in domain decomposition methods. In *Modern methods in scientific computing and applications (Montréal, QC, 2001)*, volume 75 of *NATO Sci. Ser. II Math. Phys. Chem.*, pages 323–364. Kluwer Acad. Publ., Dordrecht, 2002.

[23] O. Steinbach and M. Windisch. Stable boundary element domain decomposition methods for the helmholtz equation. *Numer. Math.*, 118(1):171–195, 2011.

[24] C. C. Stolk. A rapidly converging domain decomposition method for the helmholtz equation. *J. Comput. Phys.*, 241:240–252, 2013.

[25] R. H. Torres and Grant V. Welland. The Helmholtz equation and transmission problems with Lipschitz interfaces. *Indiana Univ. Math. J.*, 42(4):1457–1485, 1993.

[26] C. Turc, Y. Boubendir, and M. K. Riahi. Well-conditioned boundary integral equation formulations and nyström discretizations for the solution of helmholtz problems with impedance boundary conditions in two-dimensional lipschitz domains. *arXiv preprint arXiv:1607.00769*, 2016.

[27] A. Vion and C. Geuzaine. Double sweep preconditioner for optimized schwarz methods applied to the helmholtz problem. *J. Comput. Phys.*, 266:171–190, 2014.

[28] L. Zepeda-Núnez and L. Demanet. The method of polarized traces for the 2d helmholtz equation. *J. Comput. Phys.*, 308:347–388, 2016.